NACA

RESEARCH MEMORANDUM

ALTITUDE INVESTIGATION OF PERFORMANCE OF TURBINE-PROPELLER ENGINE AND ITS COMPONENTS

By Lewis E. Wallner and Martin J. Saari

Lewis Flight Propulsion Laboratory
Cleveland, Ohio

NATIONAL ADVISORY COMMITTEE FOR AERONAUTICS

WASHINGTON
October 5, 1950

NATIONAL ADVISORY COMMITTEE FOR AERONAUTICS

RESEARCH MEMORANDUM

ALTITUDE INVESTIGATION OF PERFORMANCE OF TURBINE-PROPELLER ENGINE AND ITS COMPONENTS

By Lewis E. Wallner and Martin J. Saari

SUMMARY

An altitude investigation of a turbine-propeller engine was conducted in the NACA Lewis altitude wind tunnel. A study was made of the over-all engine performance, the engine components, and the windmilling and starting characteristics.

Engine performance data obtained at sea-level static conditions could be used to predict static performance at altitudes up to 35,000 feet by use of the standard generalized parameters. Compressor, combustion-chamber, and turbine performances were unaffected by changes in altitude and were functions only of corrected engine speed, corrected fuel-air ratio, and corrected turbine speed, respectively.

Specific fuel consumption based on shaft horsepower decreased as the turbine-inlet temperature was raised at a given engine speed. The jet thrust was inappreciably affected by changes in turbine-inlet temperature at a constant engine speed but increased directly with engine speed at a constant turbine-inlet temperature. Maximum windmilling speeds were obtained at all altitudes for a propeller-blade angle of about 12°. The minimum windmilling speed at which a successful start and acceleration could be accomplished increased from 5000 rpm at an altitude of 25,000 feet to 10,000 rpm at an altitude of 40,000 feet.

INTRODUCTION

In the design of aircraft employing turbine-type power plants, a knowledge of engine performance characteristics for a wide range of flight conditions is desirable. Experimental engine performance evaluations can usually be made with relative ease and economy only at sea-level static conditions. Prediction of engine

performance at other altitudes from data obtained at sea level by use of generalized parameters is questionable unless the effects of changes in altitude on the performance of each component and the interaction of the components are known. A derivation of performance parameters for gas-turbine engines and the applicability of the parameters in generalizing the performance with changes in altitude of a turbojet engine are presented in reference 1. An investigation of the suitability of the parameters for generalizing the performance of a turbine-propeller engine is, however, necessary.

An axial-flow-compressor turbine-propeller engine has been investigated in the NACA Lewis altitude wind tunnel to study the over-all performance of the engine under altitude conditions and to evaluate individually the performance of the compressor, the combustion chambers, the turbine, the induction system, and the exhaust system operating as integral parts of the engine. Data were obtained for a range of engine operating conditions at altitudes from 5000 to 35,000 feet and a compressor-inlet ram pressure ratio of 1.00.

Results presented herein show the altitude performance of the turbine-propeller engine and its components and the applicability of the generalization method for predicting engine and component performance at altitudes other than the test altitude. The division of energy between the turbine and the jet and the performance of the induction and exhaust systems are discussed. Data from a brief investigation of windmilling and altitude starting characteristics of the engine are also presented.

DESCRIPTION OF ENGINE AND COMPONENTS

Engine. - The main engine components are a 14-stage axial-flow compressor, nine cylindrical combustion chambers, a single-stage turbine, an exhaust cone, and a planetary reduction gear (fig. 1). The maximum over-all diameter is 37 inches; the length including the exhaust cone but without the propeller is 116 inches. Dry weight of the engine plus accessories is approximately 1980 pounds. The engine has a static sea-level military rating of 1700 shaft horsepower with 550 pounds jet thrust at an engine speed of 13,000 rpm and a turbine-outlet gas temperature of 1265° F.

Air enters the engine through a screened annular inlet surrounding the aft reduction-gear casing (station 2, fig. 1). The air travels through the 14-stage compressor with a resultant

increase in pressure and temperature. Air is discharged from the compressor through two sets of guide vanes and is turned 180° before entering the combustion chambers (stations 3 and 4, fig. 1).

Most of the air flows directly into the combustion chambers and a small part is directed through the hollow turbine-nozzle vanes before entering the combustion zone. Fuel is admitted to each of the combustion chambers by means of a duplex fuel nozzle. Spark plugs are installed in two of the combustion chambers, and cross-fire tubes are provided to ignite the other chambers.

Products of combustion leaving the combustion chambers pass through transition sections to the annular turbine nozzle where the gas is accelerated. (See fig. 1, station 5.) A large part of the energy of the high-velocity gases is absorbed by the turbine to drive the compressor, the accessories, and the propeller shaft through the reduction gears. The gases are discharged from the turbine into an annular exhaust cone and through a tail pipe and jet nozzle that converts the remaining pressure energy into kinetic energy.

The turbine shaft drives the compressor directly and the propeller through the reduction-gear assembly, which consists of two planetary gear systems in series, with a speed-reduction ratio of 11.35:1. The ring gear of the high-speed stage is the floating type and its motion is restrained by six hydraulic pistons that provide a means of determining the shaft torque.

Engine components. - The compressor is a 14-stage axial-flow type with a sea-level air-flow rating of 21 pounds per second at an engine speed of 13,000 rpm. The hub- to tip-diameter ratio of the rotor (fig. 2) increases from 0.73 at the first rotor stage to 0.88 at the fourteenth rotor stage. The diameter of the rotor measured from the blade tips is $16\frac{1}{2}$ inches, and the length is 25 inches.

The engine has nine cylindrical counterflow combustion chambers (fig. 3). Air enters an annular passage in the combustion chamber, which is formed by the chamber casing and an inner liner. The casing (fig. 3(a)), which measures 6 inches in diameter and $14\frac{1}{2}$ inches in length, contains a liner (fig. 3(b)) that separates the combustion zone from the passage for the entering air flow. Openings in the liner wall allow air to pass into the combustion zone, where it is mixed with fuel sprayed from an atomizing nozzle located in the center of the combustion-chamber dome.

The over-all diameter of the turbine wheel (fig. 4) is 28 inches. The turbine blades, which are welded to the wheel rim, are 1.6 inches long and the blade chord tapers from 1.0 at the root to 0.75 inch at the tip. The turbine nozzle has an actual flow area of approximately 25 square inches and consists of 36 equally spaced hollow-steel vanes welded to inner and outer shroud rings. A portion of the air that enters the combustion chambers first flows through the hollow vanes to provide cooling. At standard sea-level conditions, the single-stage turbine can deliver approximately 5000 horsepower to the compressor and the propeller. Attached to the exhaust cone was a cylindrical tail pipe 8 feet in length and 14 inches in diameter.

APPARATUS AND INSTALLATION

The altitude wind tunnel in which the engine was investigated is a closed-throat return-flow tunnel with a test section 20 feet in diameter and 40 feet long. Pressure altitudes as high as 50,000 feet and temperatures as low as -48° F can be obtained.

The engine was installed in a streamlined nacelle-wing combination that was supported in the test section by the tunnel balance frame. (See figs. 5 and 6.) The propeller with which the engine was equipped was 12 feet 7 inches in diameter. Air was supplied to the engine from the tunnel air stream through two wing ducts with leading-edge inlets in the propeller slipstream. (See figs. 5 and 6(b).) The centers of the inlets were located at approximately 80 percent of the propeller radius. Air entering the wing ducts was turned 90° with the aid of guide vanes, as shown in figure 5. A small portion of the inlet air was diverted through bleedoff tubes for engine-nacelle cooling. At the engine, the wing ducts were joined to form an annulus around the aft reduction-gear casing.

In order to evaluate the component performance, instrumentation for measuring pressures and temperatures was placed at eight stations throughout the engine as shown in figure 1. The position of the instrumentation at six measuring stations, used in the calculation of the data, is shown in figure 7. The temperatures were automatically recorded with self-balancing potentiometers, and pressures were measured with liquid-filled multimanometer banks and were photographically recorded.

Shaft horsepower was determined from a calibration of torquemeter pressure, and jet thrust was calculated from pressure and

temperature measurements at the jet-nozzle outlet. Fuel flow to the engine was measured by a rotameter, and air flow was determined from pressure and temperature measurements at the compressor inlet.

PROCEDURE

Data were obtained for a range of engine speeds from 8000 to 13,000 rpm at altitudes from 5000 to 35,000 feet at a compressor-inlet ram pressure ratio of 1.00. Ram pressure ratio is defined as the ratio of compressor-inlet total pressure to free-stream static pressure. In order to maintain a constant ram pressure ratio at the compressor inlet, varying the tunnel air velocity was necessary to compensate for changes in duct losses and pressure rise across the propeller blades. At each altitude and engine speed, data were obtained over a range of shaft horsepowers by varying the propeller-blade angle. Ambient-air temperatures in the tunnel test section were maintained at approximately NACA standard altitude temperatures.

Symbols and methods used in calculating engine and component performance are presented in the appendix.

RESULTS AND DISCUSSION

The results obtained in this investigation are presented and discussed to show: (1) the effects of changes in engine speed and altitude on over-all engine performance; (2) the applicability of generalized parameters for predicting engine performance; (3) the effects of changes in engine speed, altitude, and turbine-inlet temperature on the division of energy between the propeller shaft and the jet; (4) the performance characteristics of each of the components operating as integral parts of the engine; and (5) the windmilling and altitude starting characteristics of the engine.

The exhaust-system pressure losses associated with the tailpipe installation used in this investigation in some cases were as high as 11 percent of the turbine-outlet total pressure. (See fig. 8.) If lower exhaust-system pressure losses had been obtained, the maximum obtainable engine power would have been higher.

Engine Performance

Engine speed. - The effect of variations in engine speed on the performance parameters at an altitude of 5000 feet is shown in figure 9. Air flow through the engine increased with an increase in engine speed, but was unaffected by changes in shaft horsepower (fig. 9(a)). The relation between shaft horsepower and turbine-inlet temperature at an altitude of 5000 feet is shown in figure 9(b) for engine speeds from 8000 to 13,000 rpm. These data were used to superimpose temperature contours on the parameters shown in figures 9(c) to 9(f). The fuel flow required to maintain a constant turbine-inlet temperature increased with engine speed (fig. 9(c)) although the fuel-air ratio decreased (fig. 9(d)). The reduction in fuel-air ratio at a given turbine-inlet temperature with increased engine speed results from the higher temperature rise across the compressor. The increase in jet thrust with engine speed at a given turbine-inlet temperature (fig. 9(e)) is rapid, which is due not only to the increased air flow but also to the larger percentage of the available total energy at the turbine inlet that remains in the gas at the turbine outlet. The variation of specific fuel consumption with shaft horsepower is shown in figure 9(f). Although the data indicate that for a given shaft horsepower the specific fuel consumption was lower at reduced engine speed, the jet thrust is not accounted for in these curves. If the specific fuel consumption were based on the total useful output of the engine, which includes the shaft horsepower and the jet thrust, the engine-speed effect shown in figure 9(f) would be minimized because the jet thrust increases with engine speed at a given value of shaft horsepower.

Altitude. - Engine performance data obtained at rated engine speed, 13,000 rpm, and altitudes from 5000 to 35,000 feet are presented in figure 10. The engine air flow was independent of the shaft horsepower but decreased approximately in proportion to the reduction of inlet-air density as the altitude was increased (fig. 10(a)). The shaft horsepower at a given altitude varied linearly with the turbine-inlet temperature, as shown in figure 10(b). The reduction in shaft horsepower with an increase in altitude at a given turbine-inlet temperature is primarily due to the reduced air flow. Contours of constant turbine-inlet temperature obtained from the data in figure 10(b) are superimposed on the other performance variables in figures 10(c) to 10(f). The fuel flow (fig. 10(c)) and the fuel-air ratio (fig. 10(d)) at a given altitude increased linearly with shaft horsepower in a manner similar to the turbine-inlet temperature. In order to obtain a given turbine-inlet temperature, a higher fuel-air ratio was required as

the altitude was raised due to the reduced compressor-inlet temperature. At each altitude the jet thrust increased slightly with shaft horsepower, as shown in figure 10(e); the increase in jet thrust was about 10 percent for an increase in shaft horsepower of 100 percent. At each altitude, the lowest value of specific fuel consumption based on shaft horsepower was obtained at the maximum temperature and power. (See fig. 10(f).) For a given turbine-inlet temperature, the minimum specific fuel consumption was obtained at altitudes between 15,000 and 25,000 feet.

Generalized Performance

Altitude performance has been generalized to standard sea-level conditions by the pressure and temperature correction factors δ and θ, respectively (reference 1). In the development of this method of generalization, these correction factors alone were not always sufficient to reduce the results completely to a single curve. The use of additional parameters, such as flight Mach number and Reynolds number, are sometimes necessary for a complete generalized description of engine-performance characteristics. (See references 2 and 3.)

Performance data obtained at a compressor-inlet ram pressure ratio of 1.00 and at altitudes from 5000 to 35,000 feet are presented in figures 11 and 12. Corrected values of fuel flow, horsepower, and jet thrust are cross-plotted at constant corrected turbine-inlet temperatures and are presented as a function of corrected engine speed in figures 11(a) to 11(c). Irrespective of the altitude at which the data were obtained, the corrected engine speed and turbine-inlet temperature define a corrected fuel flow, horsepower, and jet thrust. The corrected fuel flow and jet thrust vary almost linearly with corrected engine speed at constant corrected turbine-inlet temperatures (figs. 11(a) and 11(c)). The corrected horsepower also varied as a direct function of the engine speed in the low range; but at higher engine speeds, the horsepower reached a maximum and then decreased with further increases in engine speed.

Corrected engine performance is presented in the form of composite curves of fuel flow and jet thrust against turbine-inlet temperature at constant values of shaft horsepower and engine speed in figures 12(a) and 12(b), respectively. By the use of these curves, complete engine performance can be estimated for static conditions at altitudes up to 35,000 feet. At altitudes higher than those investigated, the changes in Reynolds number at

the inlet of the compressor would probably lessen the possibility of the data reducing to a single curve. (See reference 2.) Hence, the accuracy of performance extrapolations from figure 12 at very high altitudes would be questionable.

Engine-Power Division

A primary consideration in the design of a turbine-propeller engine is the division of power between the propeller shaft and the jet. This division of power is important not only to the maximum thrust or power obtainable at any flight condition but also to the operating economy of the engine. The division of power can be expressed as the ratio of equivalent propeller-shaft enthalpy drop to total available enthalpy drop and as the ratio of jet enthalpy drop to total available enthalpy drop. The method of calculating these ratios is given in the appendix. The shaft and jet enthalpy drop ratios are shown as functions of corrected turbine-inlet temperature in figure 13 for several corrected engine speeds and altitudes. At all corrected engine speeds the shaft enthalpy drop ratio increased, whereas the jet enthalpy drop decreased with an increase in corrected turbine-inlet temperature. An increase in corrected engine speed from 10,200 to 13,250 rpm at a constant corrected turbine-inlet temperature of 1900° R reduced the shaft enthalpy drop ratio from 0.31 to 0.22 and increased the jet enthalpy drop ratio from 0.09 to 0.13 (fig. 13(a)). The reduction in shaft enthalpy drop ratio with increased engine speed can be attributed to the increase in exhaust-system pressure losses and to the increase in the percentage of total turbine power absorbed by the compressor. Changes in altitude at constant corrected engine speed had no appreciable effect on the enthalpy drop ratios (fig. 13(b)).

With an engine having a fixed-area exhaust nozzle, such as the one investigated, a single propeller shaft power is obtained for a particular engine speed and turbine-inlet temperature. Operation at different power ratios for cruise and high-speed flight may, however, be desirable so that a range of engine powers could be obtained at a given engine speed and turbine-inlet temperature. A variable-area exhaust nozzle would provide the necessary flexibility in the engine operating characteristics.

Component Performance

Compressor. - The over-all performance characteristics of a compressor are usually represented by the variation of compressor

pressure ratio with corrected air flow at constant corrected engine speeds. Such characteristics are generally obtained by varying the pressure ratio at each engine speed from the lowest feasible value to the value limited by compressor stall. Because the compressor was investigated as an integral part of an engine, the range of pressure ratios obtainable was limited to those encountered in the normal operation of the engine.

The variation of corrected air flow with corrected engine speed is shown in figure 14. Each cluster of data points was obtained by increasing the shaft horsepower at a given engine speed with an attendant increase in compressor pressure ratio. Such variations in the compressor pressure ratio had no apparent effect on the corrected air flow. For the range of conditions investigated, the relation between corrected air flow and corrected engine speed was unaffected by changes in altitude.

Data are presented in figure 15 to show the variation of compressor pressure ratio with the square root of the corrected turbine-inlet temperature for several values of corrected air flow. At each value of corrected air flow, the relation between the two variables presented is linear because the velocity in the turbine nozzles is sonic. When the velocity through the turbine nozzles becomes sonic, the compressor pressure ratio is related to the turbine temperature ratio in the following manner, which is derived in the appendix:

$$\frac{P_3}{P_2} \propto \sqrt{\frac{T_5}{T_2}} \propto \sqrt{\frac{T_5}{\theta}} \qquad (A12)$$

In order to determine the effect of changes in altitude on the efficiency of the compressor, compressor pressure and temperature ratios were plotted as a function of the corrected turbine-inlet temperature. These curves (similar to fig. 15) were then cross-plotted to obtain the variation of compressor pressure and temperature ratios with corrected engine speed (fig. 16). Because the cross-plotted data for the altitude range investigated determined a single curve for each corrected turbine-inlet temperature, it was concluded that the compressor efficiency was unaffected by changes in altitude.

Over-all performance of the compressor is represented by the generalized characteristic curves shown in figure 17. Constant-corrected-engine-speed lines, which were obtained by varying the turbine power at each engine speed, are shown with efficiency contours obtained from cross plots of the data. Several operating

lines at constant corrected turbine-inlet temperature are superimposed on the characteristic curves. These data represent compressor operation from corrected engine speeds of 8200 to 14,200 rpm and corrected turbine-inlet temperatures from 1600° to 2400° R, which include the entire range of compressor operation in the engine. Operation of the engine at a corrected speed of 13,000 rpm, which corresponds to rated speed at sea level, occurred in the region of maximum compressor efficiency. The compressor efficiencies obtained may be somewhat low because of the dirt and oil deposits that accumulated on the rotor and stator blading during the investigation. Large changes in compressor pressure ratio at rated engine speed, induced by variations in turbine-inlet temperature, resulted in only a small change in compressor efficiency. Operation at rated engine speed as the altitude was increased from approximately 5000 to 25,000 feet resulted in a reduction of compressor efficiency of about 2 percent because the corrected engine speed increased from 13,250 to 14,200 rpm. The lowest efficiency contour obtained with the engine operating (69 percent) was extended by use of windmilling compressor data.

Combustion chamber. - The loss in total pressure across the combustion chamber of a turbine-propeller engine is attributed to two sources: the friction pressure loss resulting from the gas passing through the combustion chamber, and the momentum pressure loss resulting from the addition of heat to the gas. (A more detailed discussion is presented in reference 4.) The sum of these two pressure losses is the measured loss in total pressure across the combustion chamber, which is expressed as the total-pressure-loss ratio $(P_3 - P_5)/P_3$. The variation of total-pressure-loss ratio with corrected combustion-chamber temperature rise for altitudes from 5000 to 35,000 feet is shown in figure 18(a). These data include operation at corrected engine speeds between 8200 and 14,200 rpm. The total-pressure-loss ratio is independent of altitude changes, but decreased slightly as the corrected temperature rise was increased. The total-pressure-loss ratio is plotted as a function of the corrected horsepower of the engine for various corrected engine speeds at an altitude of 5000 feet in figure 18(b). At a constant power output, increasing the engine speed results in a higher total-pressure-loss ratio because of the lower combustion-chamber temperature rise required at the higher engine speed. The decrease in the total-pressure-loss ratio with increased temperature rise (fig. 18(a)) is a result of the reduction in Mach number entering the combustion chamber. This reduction in the Mach number decreases the friction pressure losses and thus the total-pressure-loss ratio.

The temperature rise across the combustion chamber for a given fuel-air ratio is a measure of the efficiency of the combustion process in an engine. In order to determine the effect of altitude on the performance

of the combustion chamber, the corrected combustion-chamber temperature rise was plotted as a function of the corrected engine fuel-air ratio in figure 19 for altitudes from 5000 to 35,000 feet. These data, which include engine operation at corrected speeds between 8200 and 14,200 rpm, indicate that the combustion process was unaffected by changes in altitude up to 35,000 feet.

Turbine. - Because the turbine was investigated as an integral part of the engine, the over-all engine characteristics limited the range of turbine operation that could be obtained. Three graphical representations are sufficient to show the performance of the turbine when operating as part of the engine. The turbine operating lines can be represented by the variation of turbine pressure ratio with corrected turbine speed for values of constant corrected turbine-inlet temperature, the variation of turbine efficiency with corrected turbine speed, and the variation of turbine pressure ratio with corrected gas flow.

The relation between corrected turbine speed and turbine pressure ratio for several fixed values of corrected turbine-inlet temperature shown in figure 20 was obtained from a plot of corrected turbine speed as a function of turbine pressure ratio and corrected turbine-inlet temperature for several constant corrected engine speeds. At a given corrected turbine-inlet temperature, the turbine pressure ratio was approximately proportional to the corrected turbine speed. The corrected turbine-speed range obtained during the investigation was between 4400 and 7800 rpm and most data were obtained at turbine pressure ratios higher than the critical value for choking of flow, approximately 1.85.

The variation of turbine efficiency with corrected turbine speed is presented in figure 21 for the entire range of altitudes and turbine-inlet temperatures investigated. A single efficiency curve was faired through all the data obtained. The turbine efficiency varied from approximately 0.75 at a corrected turbine speed of 4400 rpm to 0.815 at a corrected turbine speed of 7500 rpm. A constant turbine efficiency of approximately 0.815 would be obtained for operation at rated engine speed from sea level to an altitude of 35,000 feet, which would correspond to corrected turbine speeds between approximately 6200 and 7500 rpm. Although considerable data scatter is indicated in figure 21, no specific altitude or turbine-inlet-temperature trends could be found.

In the presentation of turbine performance, the usual practice is to show the variation of turbine pressure ratio with corrected turbine gas flow $\frac{W_g\sqrt{\theta_5}}{\delta_5\ \gamma_5/1.4}$, as presented in figure 22. After

the velocity in the turbine nozzles becomes sonic, the value of corrected gas flow remains constant except for a possible slight effect due to changes in the ratio of specific heats; the derivation of this expression is shown in the appendix. For turbine pressure ratios above 1.85, the corrected gas flow was constant; below this value, however, where the velocity in the turbine nozzles was subsonic, the gas flow decreased.

Induction system. - Induction-system pressure losses in terms of the tunnel velocity pressure q_0 are shown as a function of the duct-inlet velocity ratio in figure 23 for altitudes from 5000 to 35,000 feet. The total-pressure-recovery factor $(P_2 - p_0)/q_0$ (which includes the total-pressure rise across the propeller) is independent of changes in altitude but varies with changes in duct-inlet velocity ratio. At the design duct-inlet velocity ratio of 0.4, which was obtained only at low engine speeds and high free-stream velocities, pressure recoveries as high as 0.90 were obtained. At the higher duct-inlet velocity ratios, however, corresponding to high engine speeds and low tunnel velocities, low pressure recoveries were obtained.

Engine Operational Characteristics

Windmilling. - Engine windmilling speeds obtained at a flight Mach number of 0.285 at altitudes from 15,000 to 35,000 feet are shown in figure 24 as a function of propeller-blade angle. At a constant propeller-blade angle and flight Mach number, the corrected engine speed was essentially independent of the altitude. Maximum engine speeds were obtained at a blade-angle setting of about 12°. Data such as that presented in figure 24 were cross-plotted to determine the maximum air velocity at which the engine could be windmilled without exceeding the speed limit of 13,000 rpm. (See fig. 25.) The need for feathering the propeller at high airspeed is evident, inasmuch as the engine overspeed limit can be exceeded at airspeeds above 275 miles per hour.

Average total and static pressures throughout the engine are shown in figure 26 for several windmilling speeds at an altitude of 35,000 feet and a propeller-blade angle of 12°. For all the windmilling speeds, a static-pressure rise occurred in the first stages of the compressor and a static-pressure drop in the last few stages. Because there is no burning in the engine combustion chamber, the compressor-outlet pressure is lowered and the last few stages act as a turbine. The increase in pressure between stations 6 and 7 is attributed to misalinement of the air flow and instrumentation at the turbine outlet.

Starting characteristics. - The problem of starting a turbine-propeller engine under static conditions is more difficult than that of a simple turbojet engine because of the additional power required to overcome the inertia of the propeller and the reduction gearing and because the self-sustaining speed of the engine is relatively high. At low altitudes the engine is accelerated with the starter motor to about 2000 rpm, at which speed the fuel and the ignition are turned on. The starter motor then assists in accelerating the engine to 5000 rpm, at which speed the engine becomes self-sustaining and the starter motor is disengaged.

Because of the decrease in air pressure and density at high altitudes, ignition is more difficult and less power is available to accelerate the engine. As a result, the minimum engine speed at which starting and acceleration can be accomplished increases with altitude. The variation of the minimum windmilling speed at which the engine can be started and accelerated with altitude is shown in figure 27. Data for altitudes below 25,000 feet are not shown inasmuch as the minimum windmilling speed for starting was within the speed range of the starter motor. The minimum windmilling starting speed increased from 5000 rpm at an altitude of 25,000 feet to 10,000 rpm at 40,000 feet. Although ignition was obtained at lower engine speeds than those indicated in figure 27, acceleration could not be accomplished. (A detailed discussion of the starting problem is presented in reference 5.)

SUMMARY OF RESULTS

A turbine-propeller engine was investigated in the NACA Lewis altitude wind tunnel to determine the altitude performance of the engine and its component parts, and the windmilling and starting characteristics. Engine performance data obtained at sea-level static conditions for the engine investigated could be used to predict static performance at altitudes up to 35,000 feet by the application of the standard air pressure and temperature correction factors. The engine performance data generalized because the generalized performances of the compressor, the combustion chambers, and the turbine were unaffected by changes in altitude and were functions only of corrected engine speed, corrected fuel air ratio, and corrected turbine speed, respectively.

Specific fuel consumption based on shaft horsepower decreased as the turbine-inlet temperature was increased at a constant engine speed. The air flow through the engine was unaffected by changes in the turbine-inlet temperature but varied directly with

the rotating speed of the engine. Jet thrust varied directly with engine speed at constant turbine-inlet temperature but was negligibly affected by changes in turbine-inlet temperature at a given engine speed. Increasing the engine speed at a given altitude lowered the portion of the total available power absorbed by the propeller shaft at a given turbine-inlet temperature. Operation of the engine at a corrected speed of 13,000 rpm, which corresponds to rated speed at sea level, occurred in the region of maximum compressor efficiency. Maximum turbine efficiency was obtained at rated engine speed for all altitudes investigated.

For the windmilling condition, highest rotating speeds of the engine were obtained at a propeller-blade angle of about 12°. At altitudes above 25,000 feet, the minimum windmilling speed at which the engine could be started and accelerated increased from 5000 rpm at an altitude of 25,000 feet to 10,000 rpm at an altitude of 40,000 feet.

Lewis Flight Propulsion Laboratory,
National Advisory Committee for Aeronautics,
Cleveland, Ohio.

APPENDIX - METHODS OF CALCULATION

Symbols

The following symbols are used in this report:

A	cross-sectional area, sq ft
a	speed of sound in air, ft/sec
c_p	specific heat of gas at constant pressure, Btu/(lb)($^\circ$R)
F_j	jet thrust, lb
F_N	net thrust, lb
f	fuel-air ratio
g	acceleration due to gravity, ft/sec^2
ghp	horsepower loss in high-speed reduction gear
H	enthalpy, Btu/lb
hp	horsepower
J	mechanical equivalent of heat, ft-lb/Btu
K,K_1	constants
M	Mach number
N	engine speed, rpm
P	total pressure, lb/sq ft
p	static pressure, lb/sq ft
q_0	free-stream dynamic pressure, lb/sq ft
R	gas constant, 53.4 ft-lb/(lb)($^\circ$R)
shp	shaft horsepower measured at torquemeter
T	total temperature, $^\circ$R

T_i indicated temperature, °R

T_3' isentropic compressor-outlet total temperature, °R

T_6' isentropic turbine-outlet total temperature, °R

t static temperature, °R

V velocity, ft/sec

W_a air flow, lb/sec

W_f fuel flow, lb/hr

W_g gas flow, lb/sec

β propeller-blade angle, deg

γ ratio of specific heats for gases

δ ratio of compressor-inlet total pressure to static pressure of NACA standard atmosphere at sea level

δ_5 ratio of turbine-inlet total pressure to static pressure of NACA standard atmosphere at sea level

η_c compressor efficiency

η_t turbine efficiency

θ ratio of compressor-inlet absolute total temperature to absolute static temperature of NACA standard atmosphere at sea level

θ_5 product of γ and total temperature at turbine inlet divided by product of γ and static temperature for air at NACA standard sea-level conditions $(\gamma_5 T_5/1.40 \times 519)$

ρ density, slugs/cu ft

Subscripts:

j jet

n turbine nozzle (minimum area)

t	turbine
0	tunnel-test-section air stream
1	wing-duct inlet
2	compressor inlet
3	compressor outlet
5	turbine inlet
6	turbine outlet
8	jet-nozzle outlet

The data are generalized to NACA standard sea-level conditions by the following parameters:

F_j/δ	corrected jet thrust, lb
f/θ	corrected fuel-air ratio
$hp/\delta\sqrt{\theta}$	corrected horsepower, shp + ghp
$N/\sqrt{\theta}$	corrected engine speed, rpm
$N/\sqrt{\theta_5}$	corrected turbine speed, rpm
T_5/θ	corrected turbine-inlet temperature, $^{\circ}R$
$(T_5 - T_3)/\theta$	corrected combustion-chamber temperature rise, $^{\circ}F$
$W_a\sqrt{\theta}/\delta$	corrected air flow, lb/sec
$W_f/\delta\sqrt{\theta}$	corrected fuel flow, lb/hr
$\frac{W_g\sqrt{\theta_5}}{\delta_5\ \gamma_5/1.4}$	corrected turbine gas flow, lb/sec

Calculations

Temperatures. - Total temperatures were obtained from thermocouple readings, a thermocouple recovery factor (0.85), and the following equation:

$$T = \frac{T_1\left(\frac{P}{p}\right)^{\frac{\gamma-1}{\gamma}}}{1 + 0.85\left[\left(\frac{P}{p}\right)^{\frac{\gamma-1}{\gamma}} - 1\right]} \qquad (A1)$$

Turbine-inlet temperatures were calculated from the enthalpy drop through the turbine and the total enthalpy at the jet-nozzle outlet. The enthalpy drop through the turbine included the power required to drive the compressor, the shaft power measured at the torquemeter, and the power loss in the high-speed reduction gear:

$$H_5 = \left[\frac{(shp + ghp)550}{W_g J}\right] + (H_3 - H_2) + H_8 \qquad (A2)$$

$$T_5 = \frac{H_5}{c_{p,5}} \qquad (A3)$$

The gear horsepower, used in calculating H_5, represents the power loss in the high-speed reduction gear and was estimated to vary from 50 horsepower at an engine speed of 13,000 rpm to 25 horsepower at 8000 rpm.

Air flow. - The engine air flow used in the performance calculations was determined from measurements at the compressor inlet. From the continuity equation,

$$W_a = \rho_2 A_2 V_2 g$$

$$= \frac{p_2 A_2}{Rt_2} V_2$$

$$= p_2 A_2 \sqrt{\frac{2\gamma_g}{(\gamma - 1)Rt_2}\left[\left(\frac{P_2}{p_2}\right)^{\frac{\gamma-1}{\gamma}} - 1\right]} \qquad (A4)$$

The gas flow through the turbine nozzles was assumed equal to the compressor-inlet air flow plus the fuel flow,

$$W_g = W_a + \frac{W_f}{3600} \tag{A5}$$

Compressor efficiency. - The compressor efficiency is defined as

$$\eta_c = \frac{\text{Isentropic enthalpy rise}}{\text{Actual enthalpy rise}}$$

$$= \frac{W_a c_p (T_3' - T_2)}{W_a c_p (T_3 - T_2)}$$

$$= \frac{T_2 \left[\left(\frac{P_3}{P_2} \right)^{\frac{\gamma-1}{\gamma}} - 1 \right]}{T_3 - T_2} \tag{A6}$$

Compressor pressure ratio. - The relation between compressor pressure ratio and corrected turbine-inlet temperature, which was referred to in the discussion of the compressor, may be derived in the following manner:

$$M = \frac{V}{a} = \frac{W_g R t}{A p \sqrt{\gamma g R t}} = \frac{W_g \sqrt{R} \sqrt{t}}{A p \sqrt{\gamma g}} \tag{A7}$$

When the static temperatures are converted to total values,

$$M = \frac{W_g}{A} \sqrt{\frac{R}{\gamma g}} \frac{\sqrt{T}}{P} \left(1 + \frac{\gamma - 1}{2} M^2 \right)^{\frac{\gamma+1}{2(\gamma-1)}} \tag{A8}$$

or

$$W_a = \frac{M A \sqrt{\frac{\gamma g}{R}} \frac{P}{\sqrt{T}}}{(1 + f) \left(1 + \frac{\gamma - 1}{2} M^2 \right)^{\frac{\gamma+1}{2(\gamma-1)}}} \tag{A9}$$

Equation (A9) rewritten for conditions at the turbine nozzles where choking occurs ($M_n = 1$),

$$W_a = \frac{A_n \sqrt{\frac{\gamma_5 g}{R}} \frac{P_5}{\sqrt{T_5}}}{(1 + f) \left(1 + \frac{\gamma_5 - 1}{2}\right)^{\frac{\gamma+1}{2(\gamma_5-1)}}} \tag{A10}$$

For corrected conditions at the inlet of the compressor,

$$\frac{W_a \sqrt{\theta_2}}{\delta_2} = \frac{A_n \sqrt{\frac{\gamma_5 g}{R}} \sqrt{\frac{T_2}{T_5}} \frac{P_5}{P_2} \frac{2116}{\sqrt{519}}}{(1 + f) \left(1 + \frac{\gamma_5 - 1}{2}\right)^{\frac{\gamma+1}{2(\gamma_5-1)}}} \tag{A11a}$$

Equation (A11a) may be written as,

$$\frac{W_a \sqrt{\theta}}{\delta} = \frac{\sqrt{\frac{T_2}{T_5}} \frac{P_3}{P_2} \frac{P_5}{P_3} A_n \sqrt{\frac{\gamma_5 g}{R}} \frac{2116}{\sqrt{519}}}{(1 + f) \left(1 + \frac{\gamma_5 - 1}{2}\right)^{\frac{\gamma_5+1}{2(\gamma_5-1)}}} \tag{A11b}$$

When the combustion-chamber total-pressure ratio, the variation in specific-heat function, and the fuel-air ratio are assumed as second-order variables, equation (A11b) can be written as,

$$\frac{W_a \sqrt{\theta}}{\delta} = \sqrt{\frac{T_2}{T_5}} \left(\frac{P_3}{P_2}\right) K \tag{A11c}$$

Therefore, at a given corrected air flow, the following relation may be assumed:

$$\frac{P_3}{P_2} \propto \sqrt{\frac{T_5}{T_2}} \propto \sqrt{\frac{T_5}{\theta}} \tag{A12}$$

Turbine efficiency. - The isentropic efficiency of the turbine may be expressed as,

$$\eta_t = \frac{\text{Actual enthalpy drop}}{\text{Isentropic enthalpy drop}}$$

$$= \frac{W_g c_{p,t}(T_5 - T_6)}{W_g c_{p,t}(T_5 - T_6')}$$

$$= \frac{(T_5 - T_6)}{T_5 \left[1 - \left(\frac{P_6}{P_5}\right)^{\frac{\gamma_t - 1}{\gamma_t}}\right]} \tag{A13}$$

Corrected turbine gas flow. - Rewriting equation (A9) gives

$$\frac{W_g\sqrt{\gamma T}}{\gamma P} = \frac{\sqrt{g}\, MA}{\sqrt{R}\left(1 + \frac{\gamma - 1}{2} M^2\right)^{\frac{\gamma+1}{2(\gamma-1)}}} \tag{A14}$$

When equation (A14) is corrected to standard sea-level conditions at station 5 (turbine inlet),

$$\frac{W_g\sqrt{\theta_5}}{\delta_5\, \gamma_5/1.4} = \frac{K_1 MA_n}{\left(1 + \frac{\gamma_5 - 1}{2} M^2\right)^{\frac{\gamma_5+1}{2(\gamma_5-1)}}} \tag{A15}$$

When the pressure ratio across the turbine nozzles exceeds the critical value, the Mach number at the minimum area is unity. The

variation in the specific-heat function for the maximum turbine-inlet temperature change is less than 0.4 percent. If the parameter on the left side of equation (A15) remains constant, choking is therefore indicated in the turbine nozzles.

Thrust. - Jet thrust is equal to the product of the mass flow and the velocity at the jet-nozzle outlet plus the incremental pressure times the jet-nozzle area.

Therefore,

$$F_j = \frac{W_g}{g} V_8 + A_8(p_8 - p_0) \qquad \text{(A16)}$$

$$= \rho_8 A_8 V_8^2 + A_8(p_8 - p_0)$$

$$= \frac{A_8}{Rg} \frac{p_8}{t_8} \left\{ \frac{2\gamma g R t_8}{(\gamma - 1)} \left[\left(\frac{P_8}{p_8} \right)^{\frac{\gamma_8 - 1}{\gamma_8}} - 1 \right] \right\} + A_8(p_8 - p_0) \qquad \text{(A17)}$$

$$= A_8 p_8 \frac{2\gamma}{\gamma - 1} \left[\left(\frac{P_8}{p_8} \right)^{\frac{\gamma_8 - 1}{\gamma_8}} - 1 \right] + A_8(p_8 - p_0) \qquad \text{(A18)}$$

The net thrust is equal to the jet thrust minus the momentum of the air at the engine inlet,

$$F_N = F_j - \left(\frac{W_a}{g} \right) (V_0) \qquad \text{(A19)}$$

The enthalpy ratios shown in figure 13 were calculated in the following manner:

$$\frac{\text{Shaft enthalpy drop}}{\text{Total enthalpy drop}} = \frac{(H_5 - H_6) - (H_3 - H_2)}{H_5 - H_j} \qquad \text{(A20)}$$

$$\frac{\text{Jet enthalpy drop}}{\text{Total enthalpy drop}} = \frac{(H_6 - H_j)}{(H_5 - H_j)} \qquad (A21)$$

where H_j represents the enthalpy of the jet based on the static temperature of the exhaust gas when $p_j = p_0$. All other enthalpies are based on total temperatures.

REFERENCES

1. Sanders, Newell D.: Performance Parameters for Jet-Propulsion Engines. NACA TN 1106, 1946.

2. Wallner, Lewis E., and Fleming, William A.: Reynolds Number Effect on Axial-Flow Compressor Performance. NACA RM E9G11, 1949.

3. Sanders, Newell D., and Behun, Michael: Generalization of Turbojet-Engine Performance in Terms of Pumping Characteristics. NACA TN 1927, 1949.

4. Pinkel, I. Irving, and Shames, Harold: Analysis of Jet-Propulsion-Engine Combustion-Chamber Pressure Losses. NACA Rep. 880, 1947. (Formerly NACA TN 1180.)

5. Howard, Alan, and Walker, C. J.: An Aircraft Gas Turbine for Propeller Drive. Mech. Eng., vol. 69, no. 10, Oct. 1947, pp. 827-835.

Station

1 Wing-duct inlet (fig. 5)
2 Compressor inlet
3 Compressor outlet
4 Compressor elbow
5 Turbine inlet
6 Turbine outlet
7 Exhaust-cone outlet
8 Jet-nozzle outlet

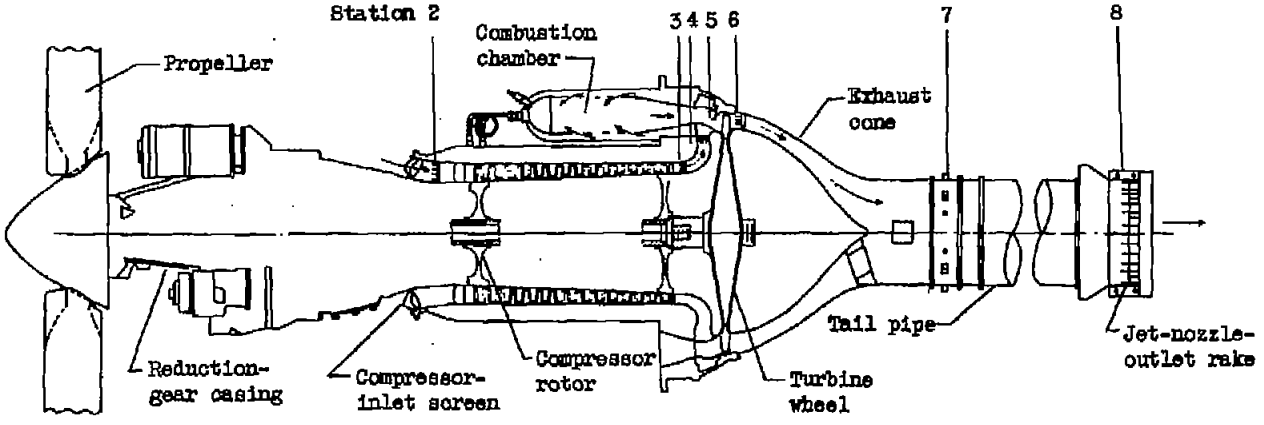

Figure 1. - Side view of turbine-propeller engine showing location of measuring stations.

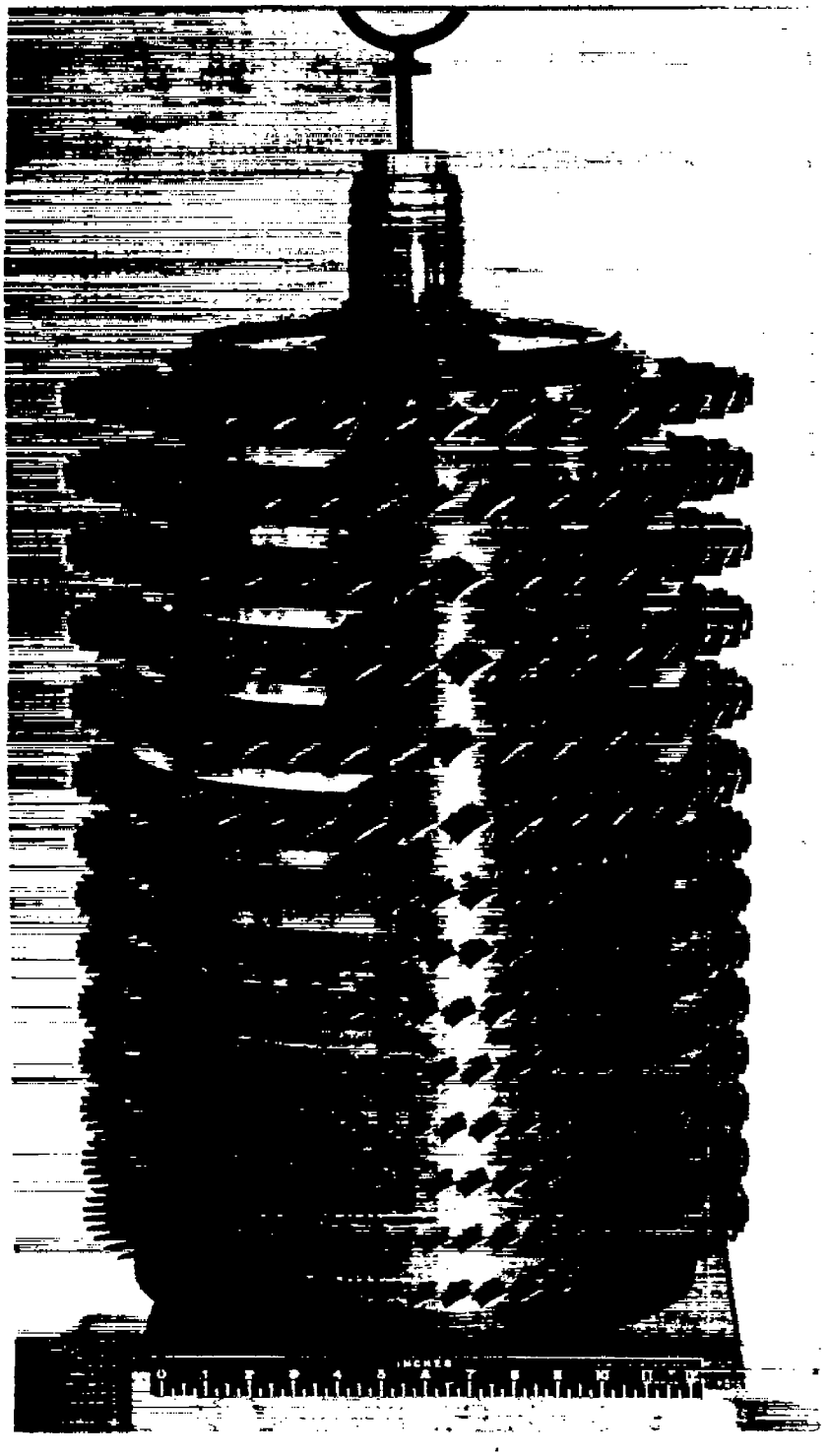

Figure 2. - Axial-flow-compressor rotor of turbine-propeller engine.

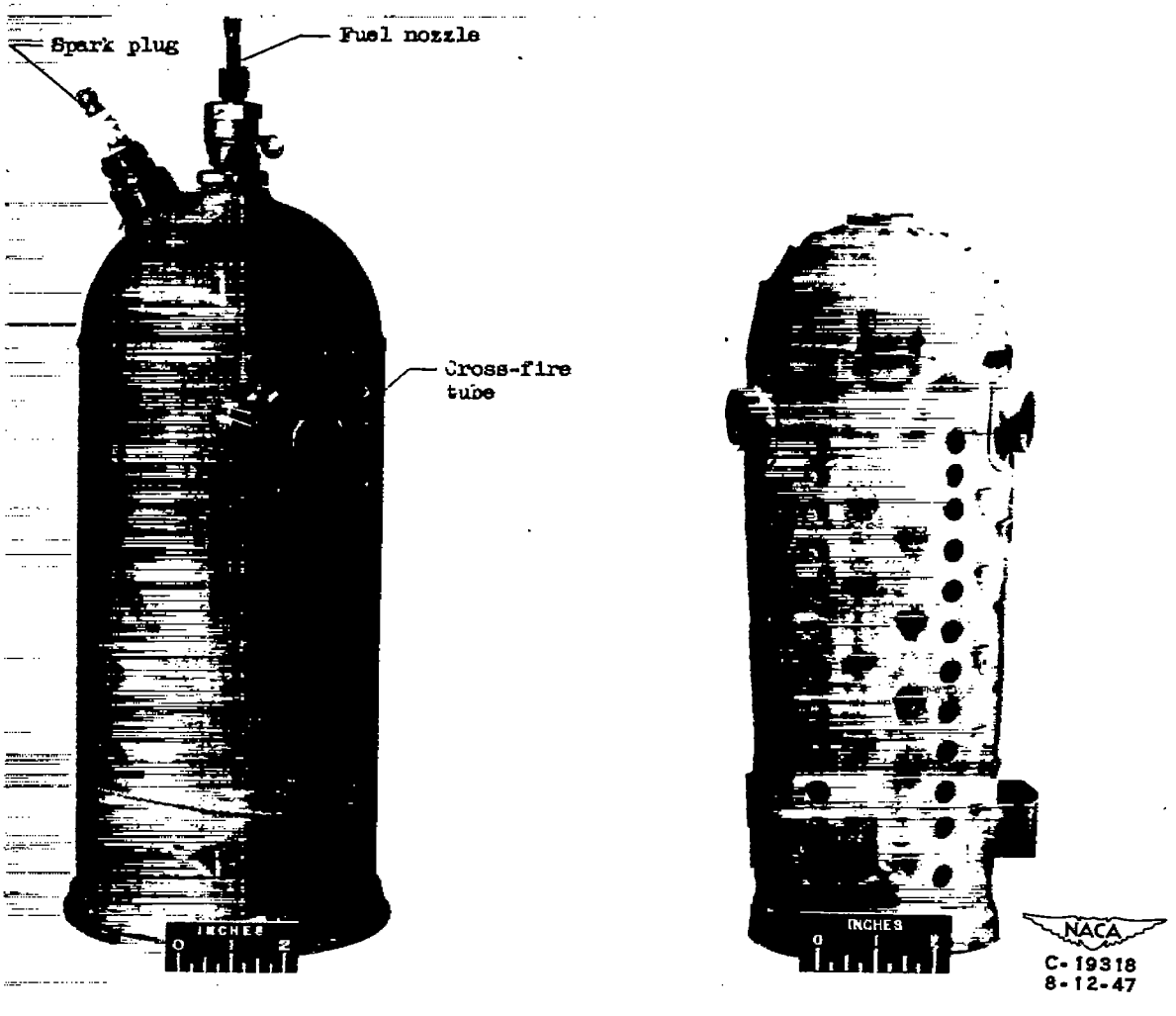

(a) Casing with spark plug installed.

(b) Liner.

Figure 3. - Counterflow combustion chamber of turbine-propeller engine.

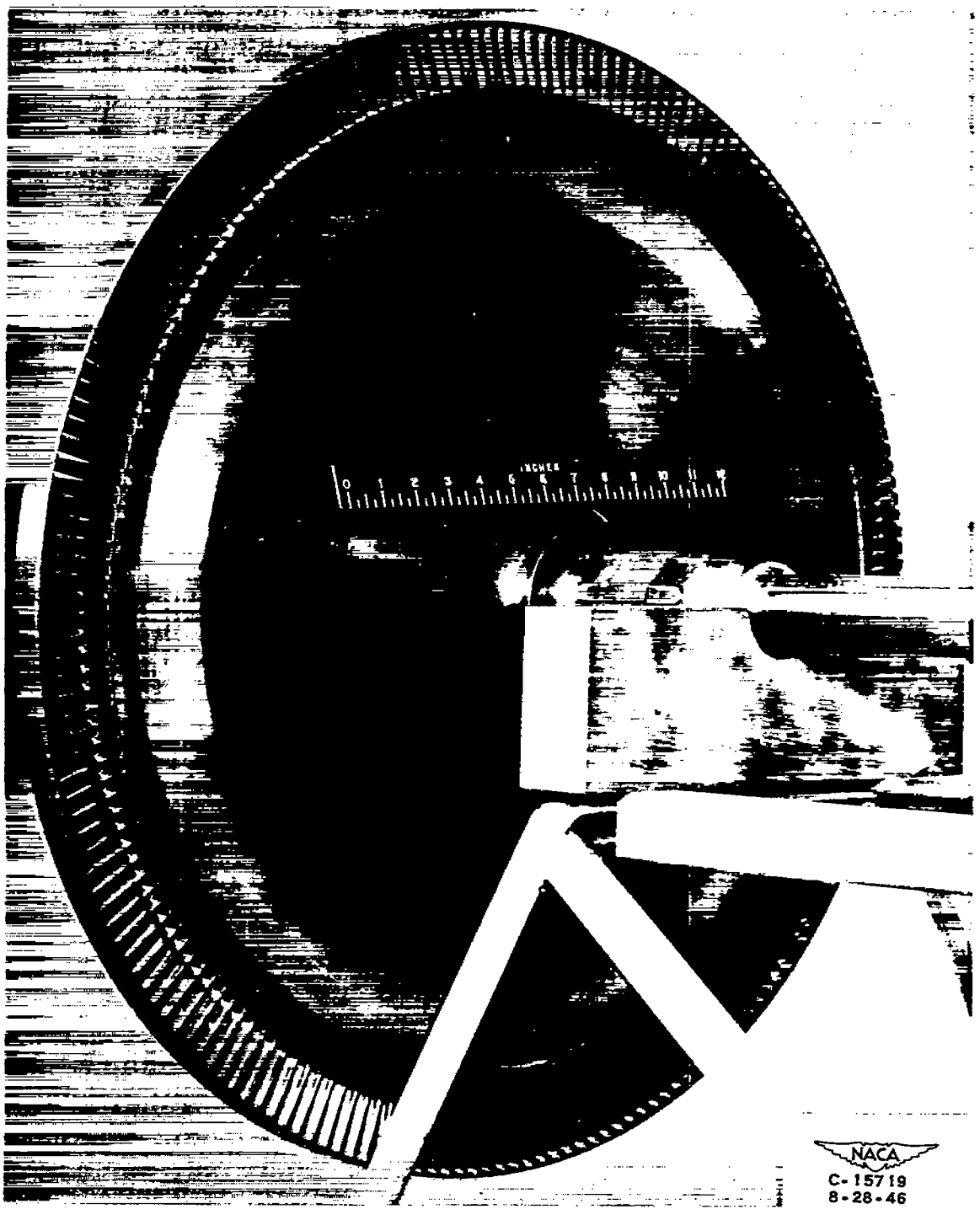

Figure 4. - Turbine wheel used in axial-flow-compressor turbine-propeller engine.

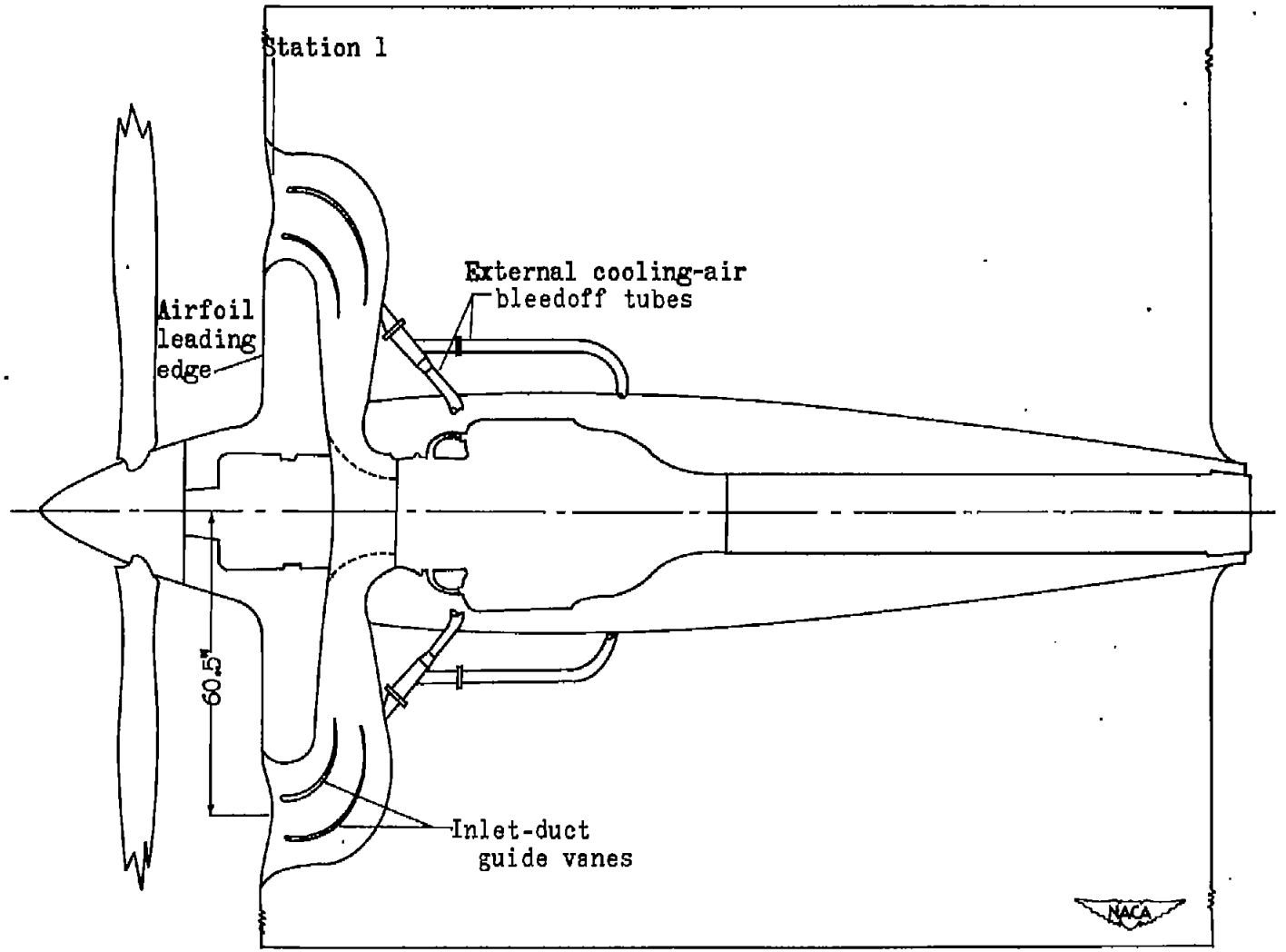

Figure 5. - Sketch of turbine-propeller-engine installation showing location of wing ducts and inlets.

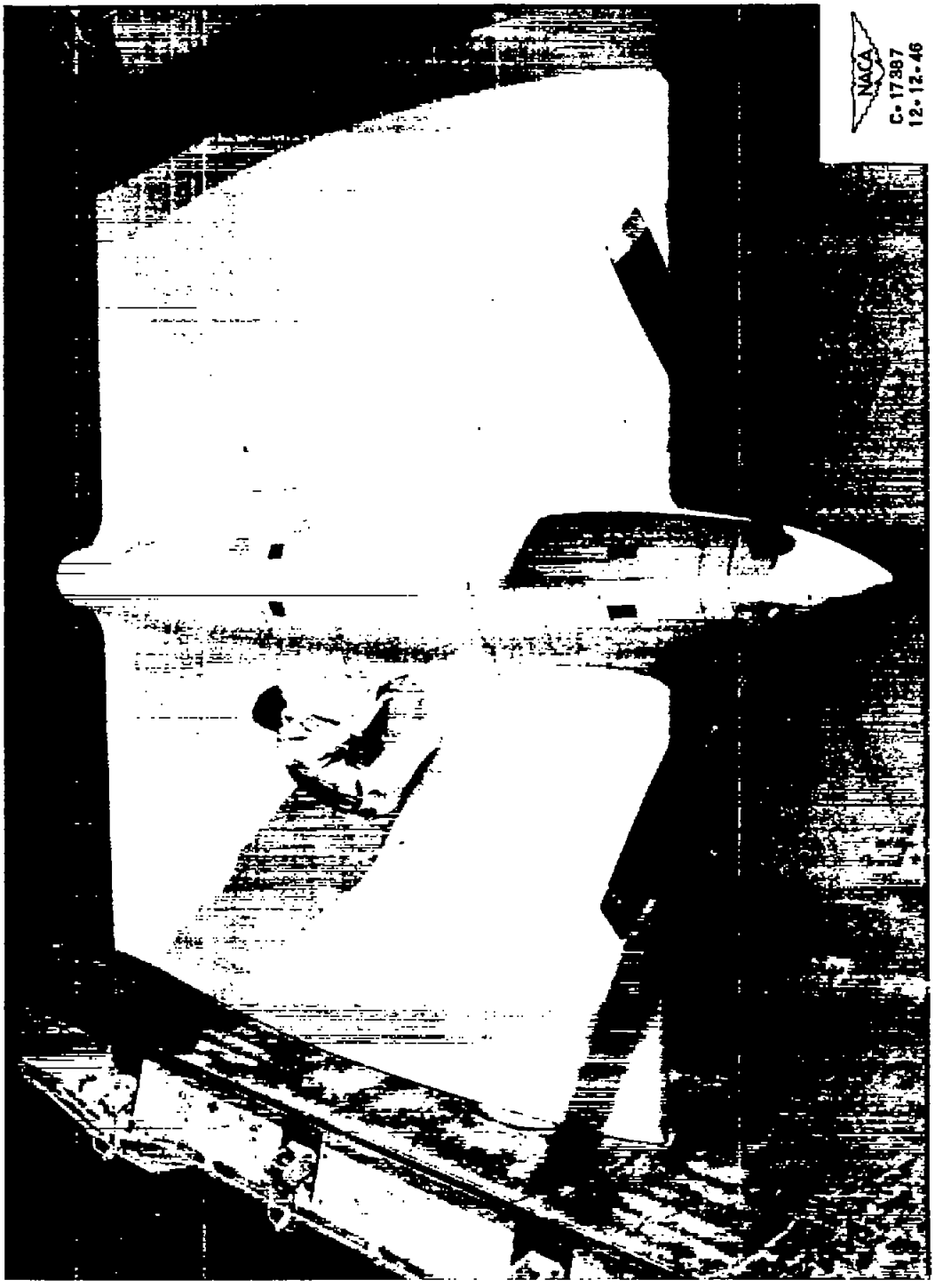

(a) Top view.

Figure 6. - Turbine-propeller engine in altitude wind tunnel.

(b) Front view.

Figure 6. - Concluded. Turbine-propeller engine in altitude wind tunnel.

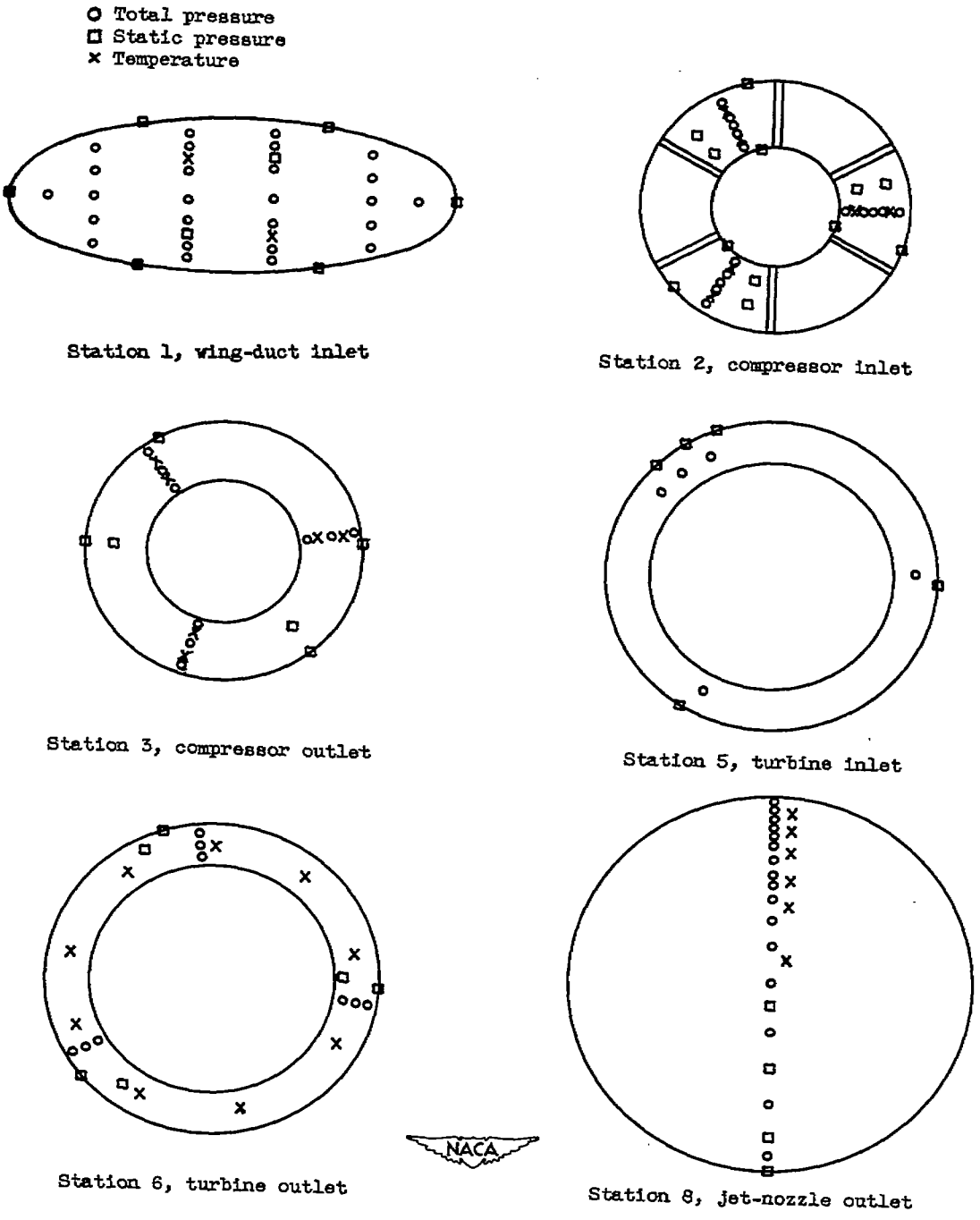

Figure 7. - Location of instrumentation for altitude-wind-tunnel investigation of turbine-propeller engine.

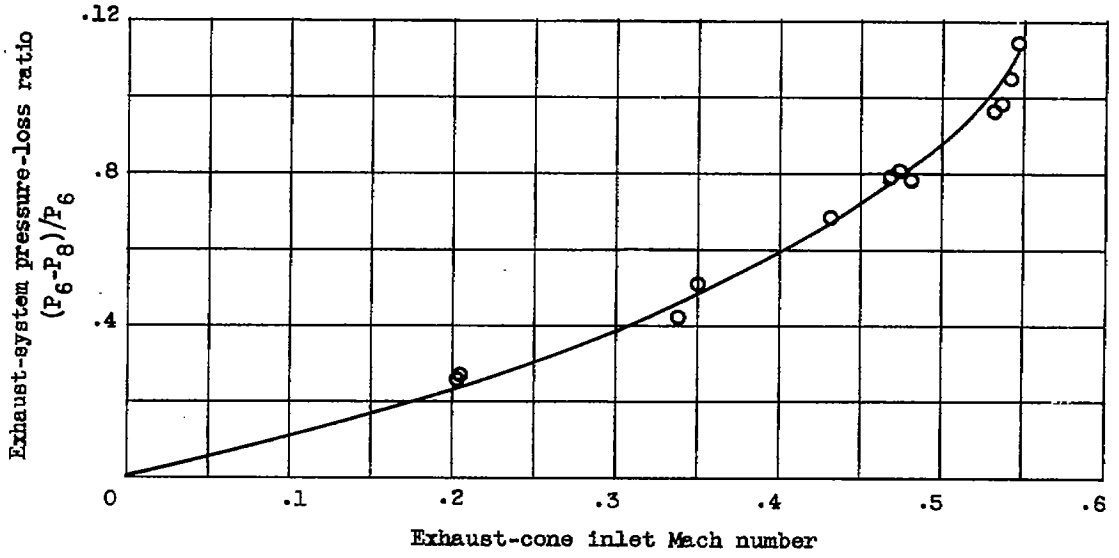

Figure 8. - Variation of exhaust-system pressure-loss ratio with exhaust-cone inlet Mach number. Exhaust-gas temperature, approximately 1500° R.

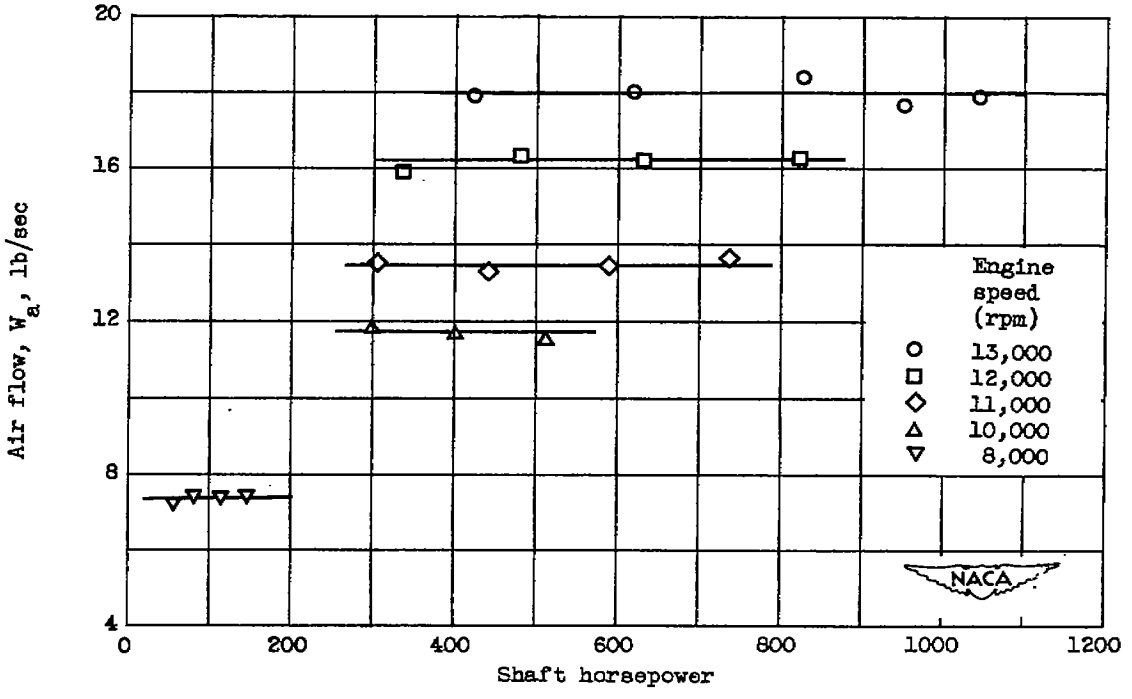

(a) Air flow.

Figure 9. - Effect of shaft horsepower on engine-performance parameters at various engine speeds. Altitude, 5000 feet; compressor-inlet ram pressure ratio, 1.00.

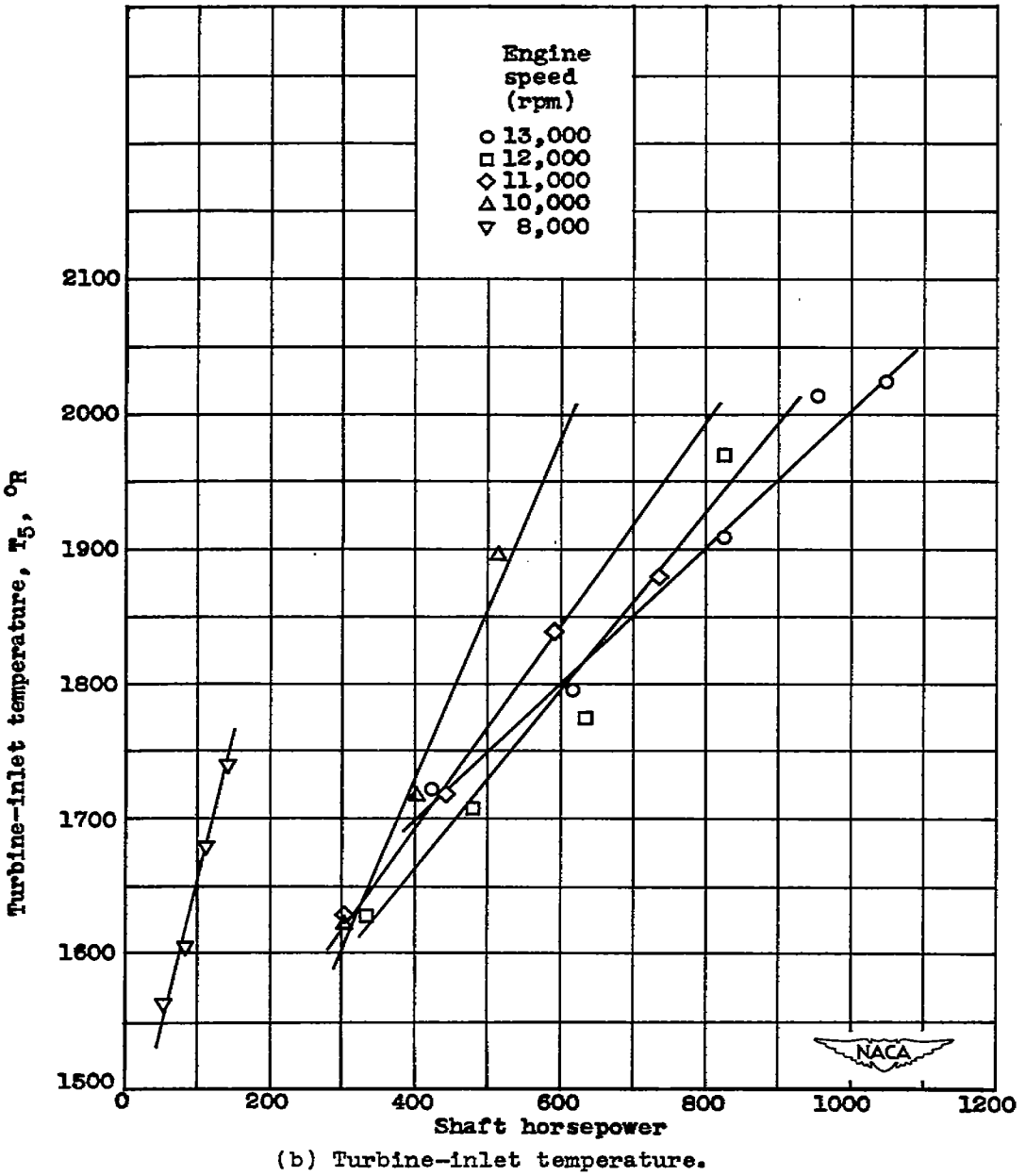

(b) Turbine-inlet temperature.

Figure 9. - Continued. Effect of shaft horsepower on engine-performance parameters at various engine speeds. Altitude, 5000 feet; compressor-inlet ram pressure ratio, 1.00.

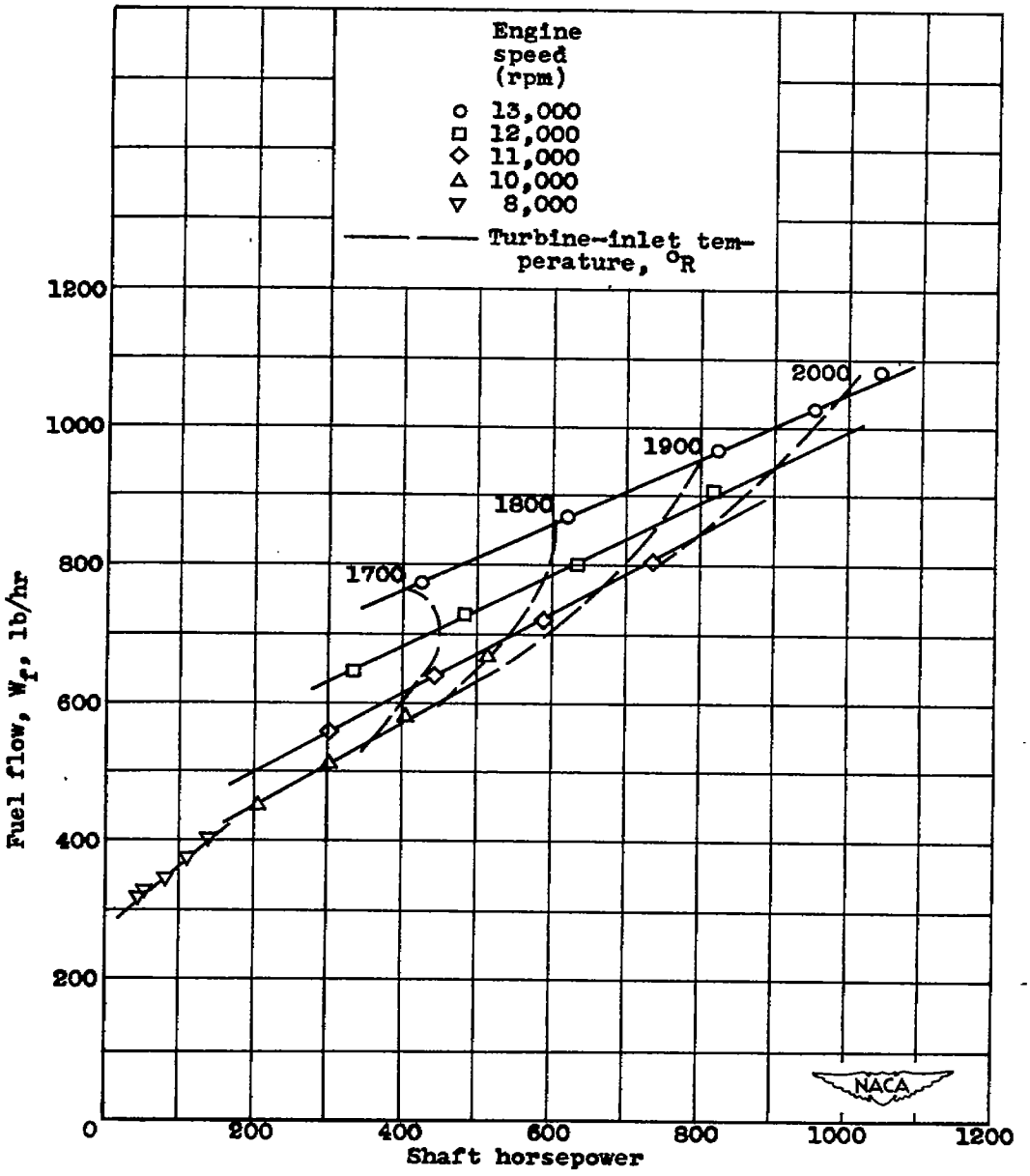

(c) Fuel flow.

Figure 9. - Continued. Effect of shaft horsepower on engine-performance parameters at various engine speeds. Altitude, 5000 feet; compressor-inlet ram pressure ratio, 1.00.

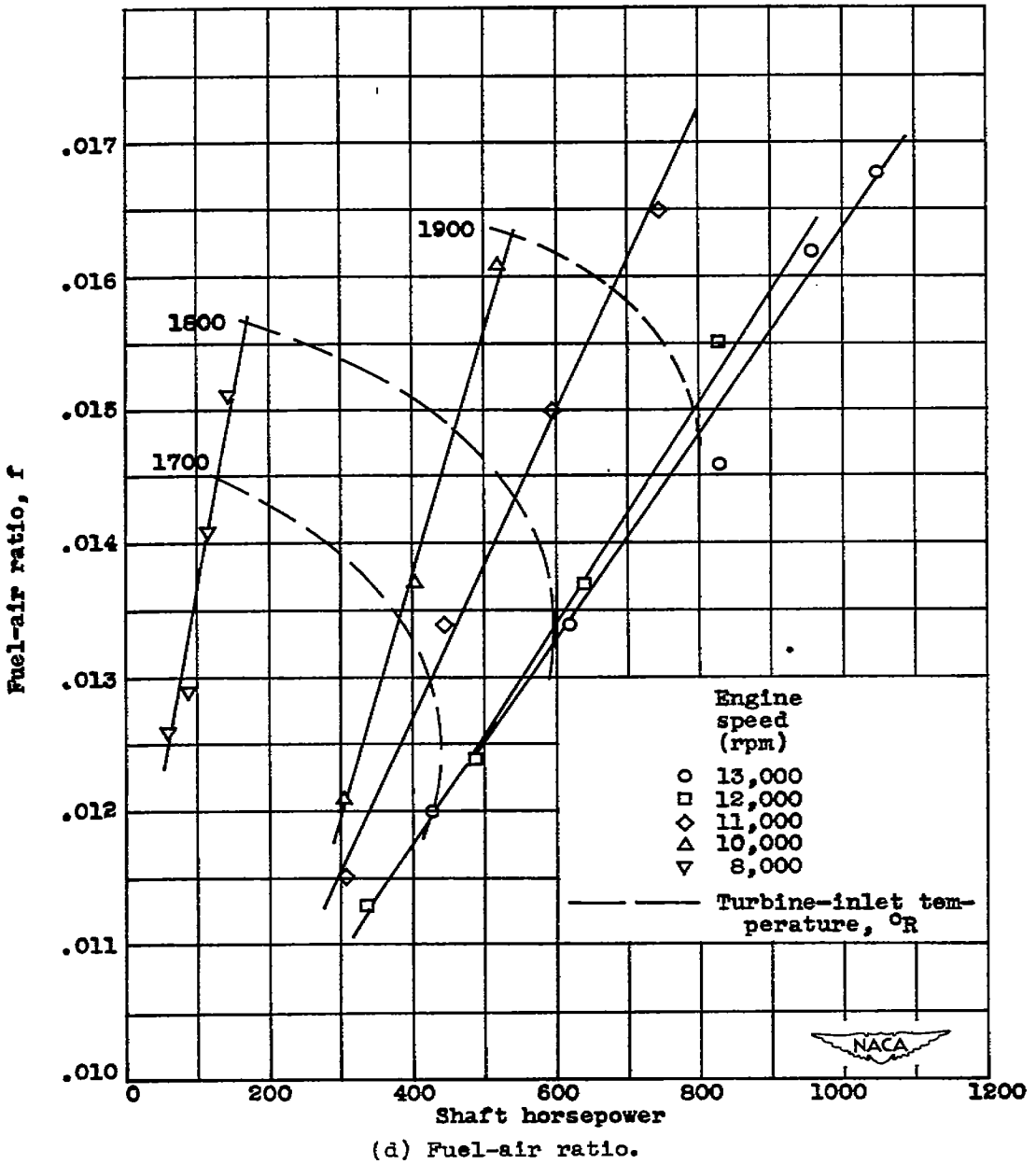

(d) Fuel-air ratio.

Figure 9. - Continued. Effect of shaft horsepower on engine-performance parameters at various engine speeds. Altitude, 5000 feet; compressor-inlet ram pressure ratio, 1.00.

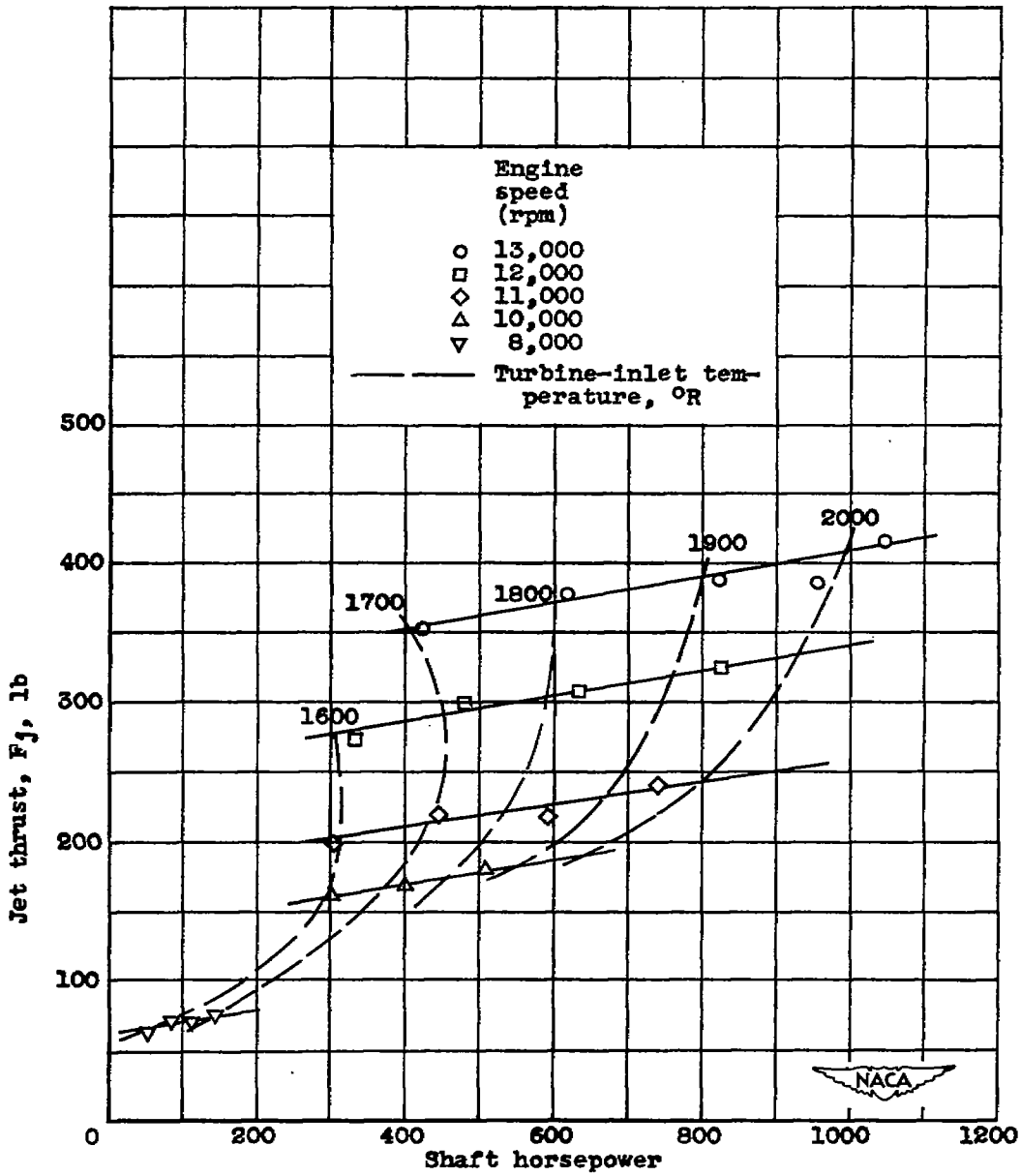

(e) Jet thrust.

Figure 9. - Continued. Effect of shaft horsepower on engine-performance parameters at various engine speeds. Altitude, 5000 feet; compressor-inlet ram pressure ratio, 1.00.

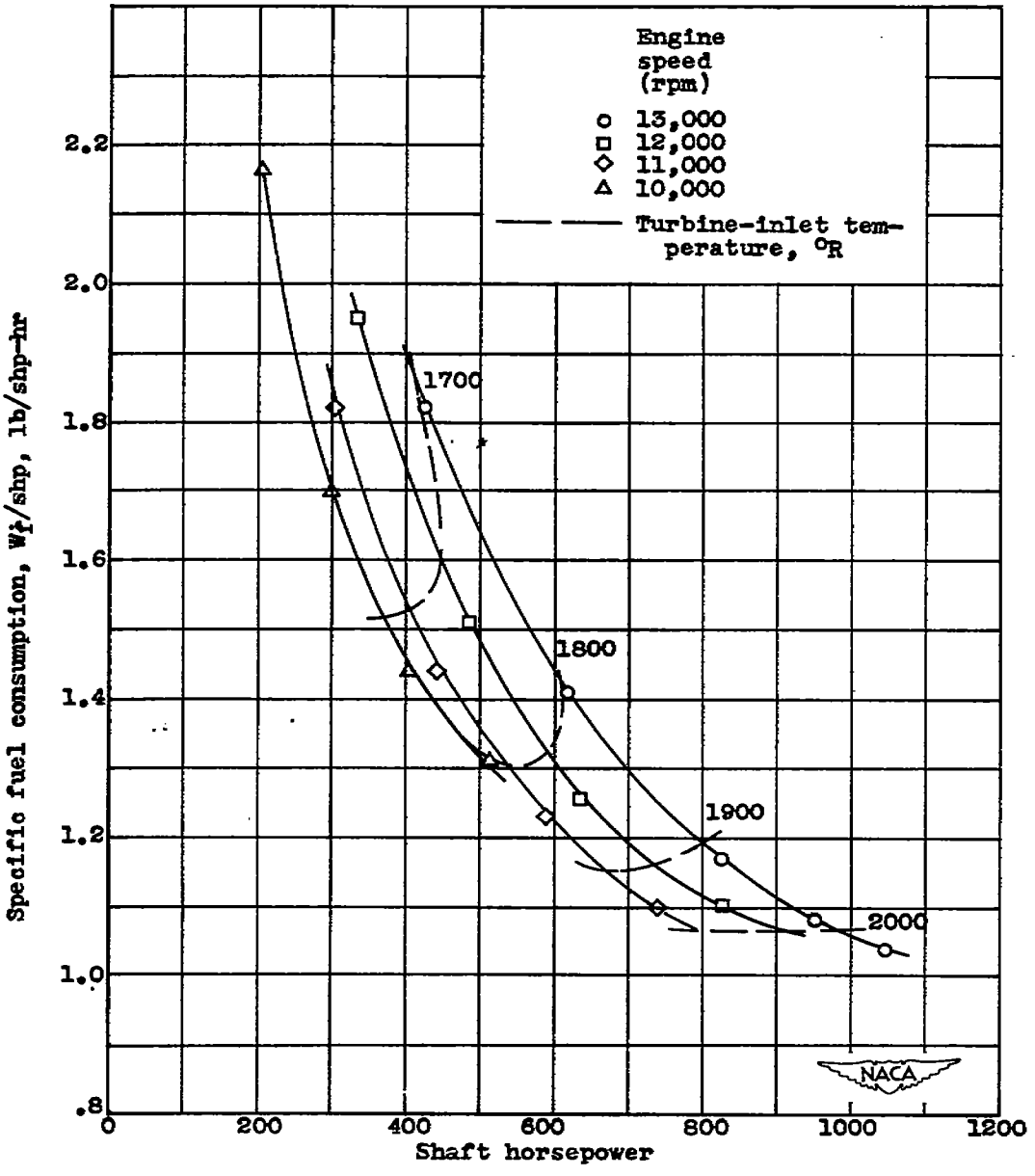

(f) Specific fuel consumption.

Figure 9. - Concluded. Effect of shaft horsepower on engine-performance parameters at various engine speeds. Altitude, 5000 feet; compressor-inlet ram pressure ratio, 1.00.

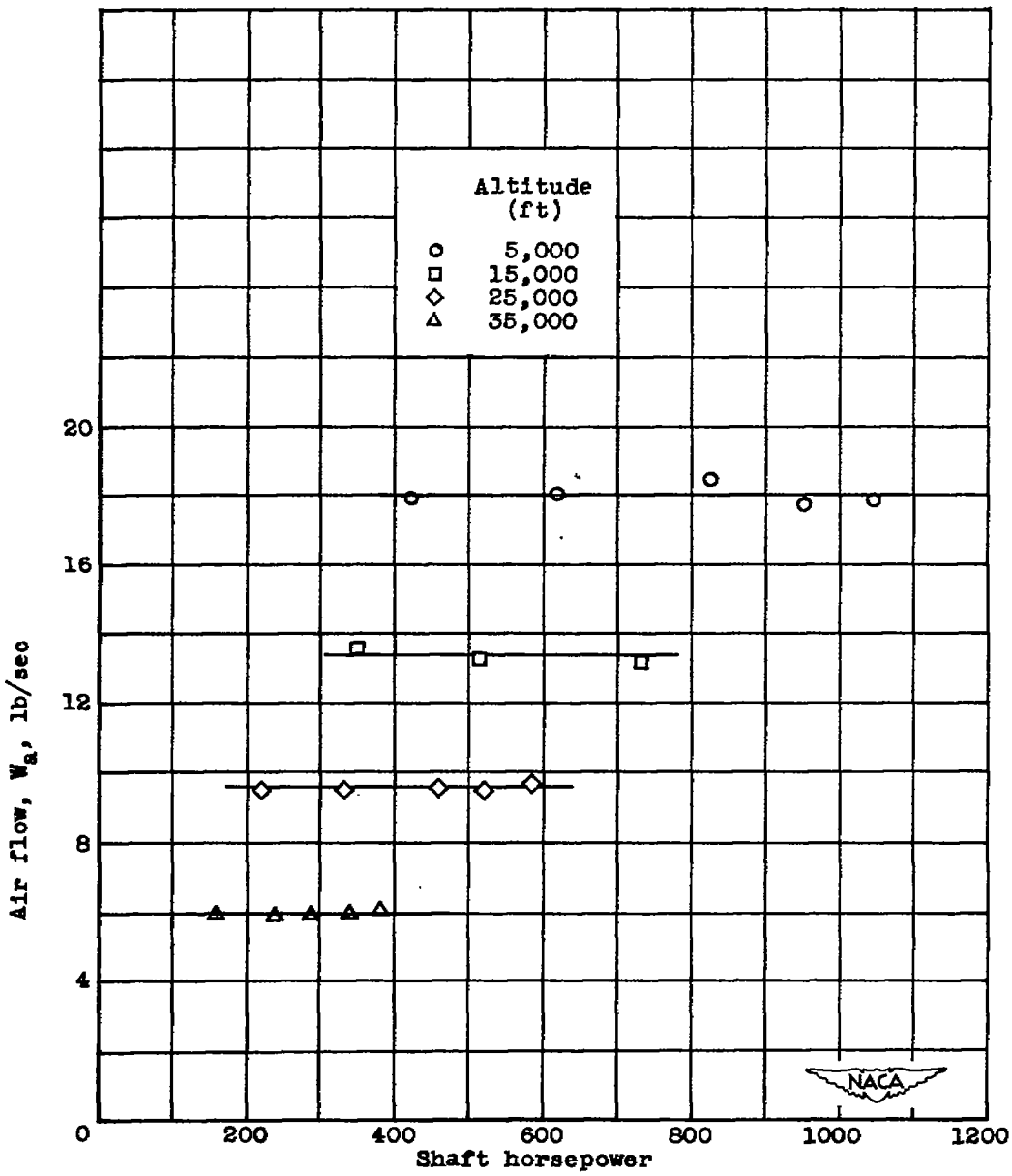

(a) Air flow.

Figure 10. - Effect of shaft horsepower on engine-performance parameters at various altitudes. Engine speed, 13,000 rpm; compressor-inlet ram pressure ratio, 1.00.

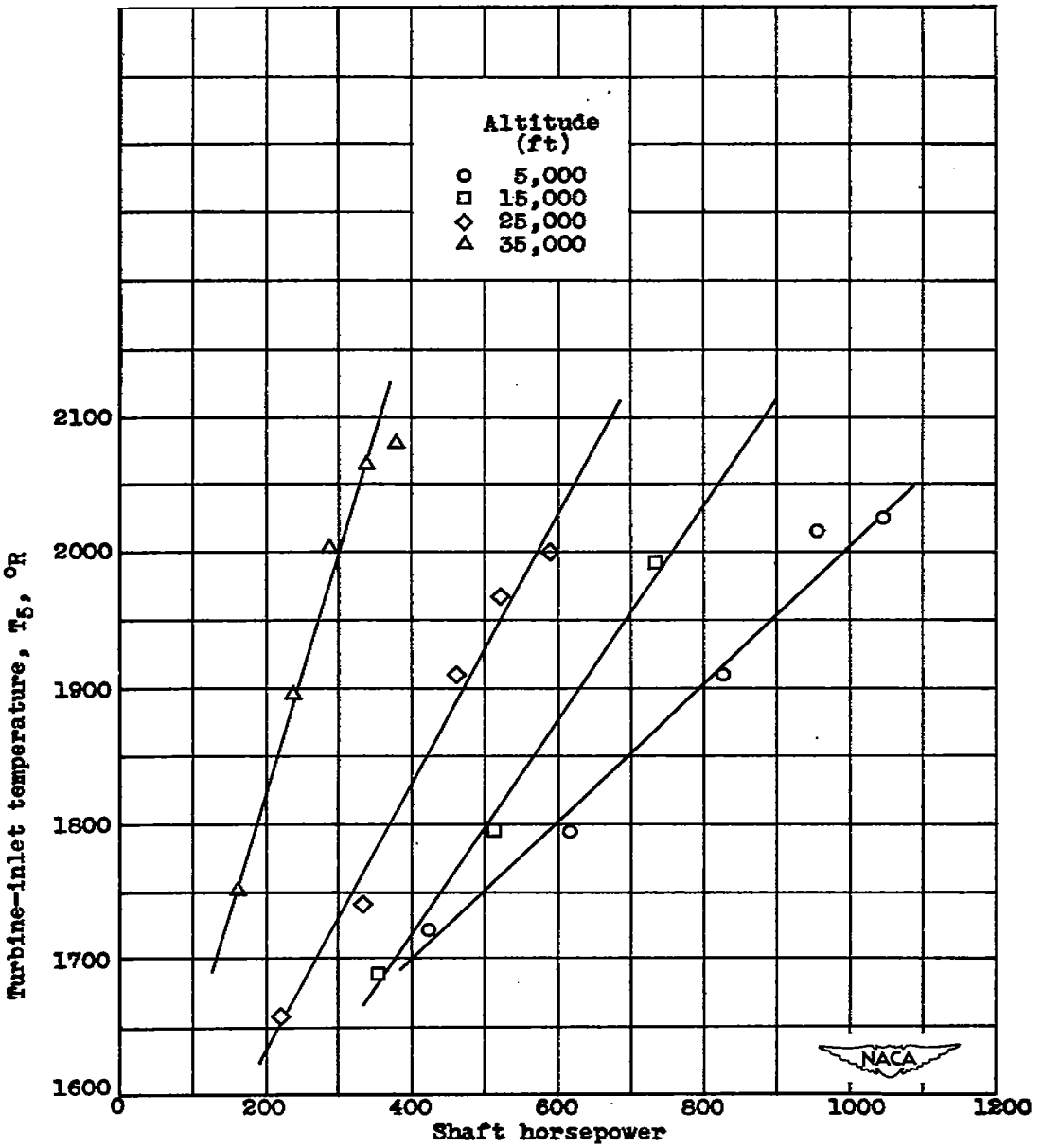

(b) Turbine-inlet temperature.

Figure 10. - Continued. Effect of shaft horsepower on engine-performance parameters at various altitudes. Engine speed, 13,000 rpm; compressor-inlet ram pressure ratio, 1.00.

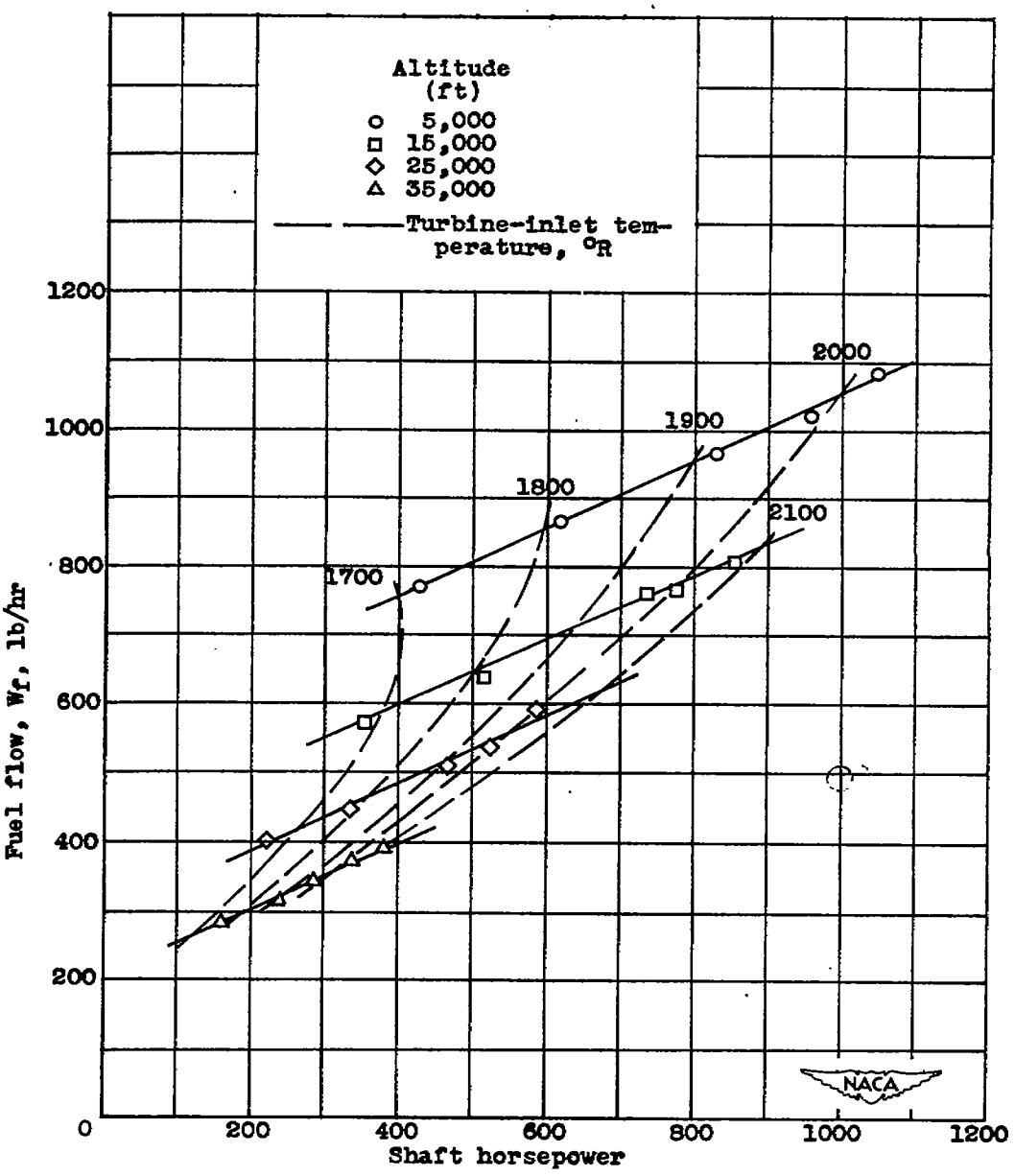

(c) Fuel flow.

Figure 10. - Continued. Effect of shaft horsepower on engine-performance parameters at various altitudes. Engine speed, 13,000 rpm; compressor-inlet pressure ratio, 1.00.

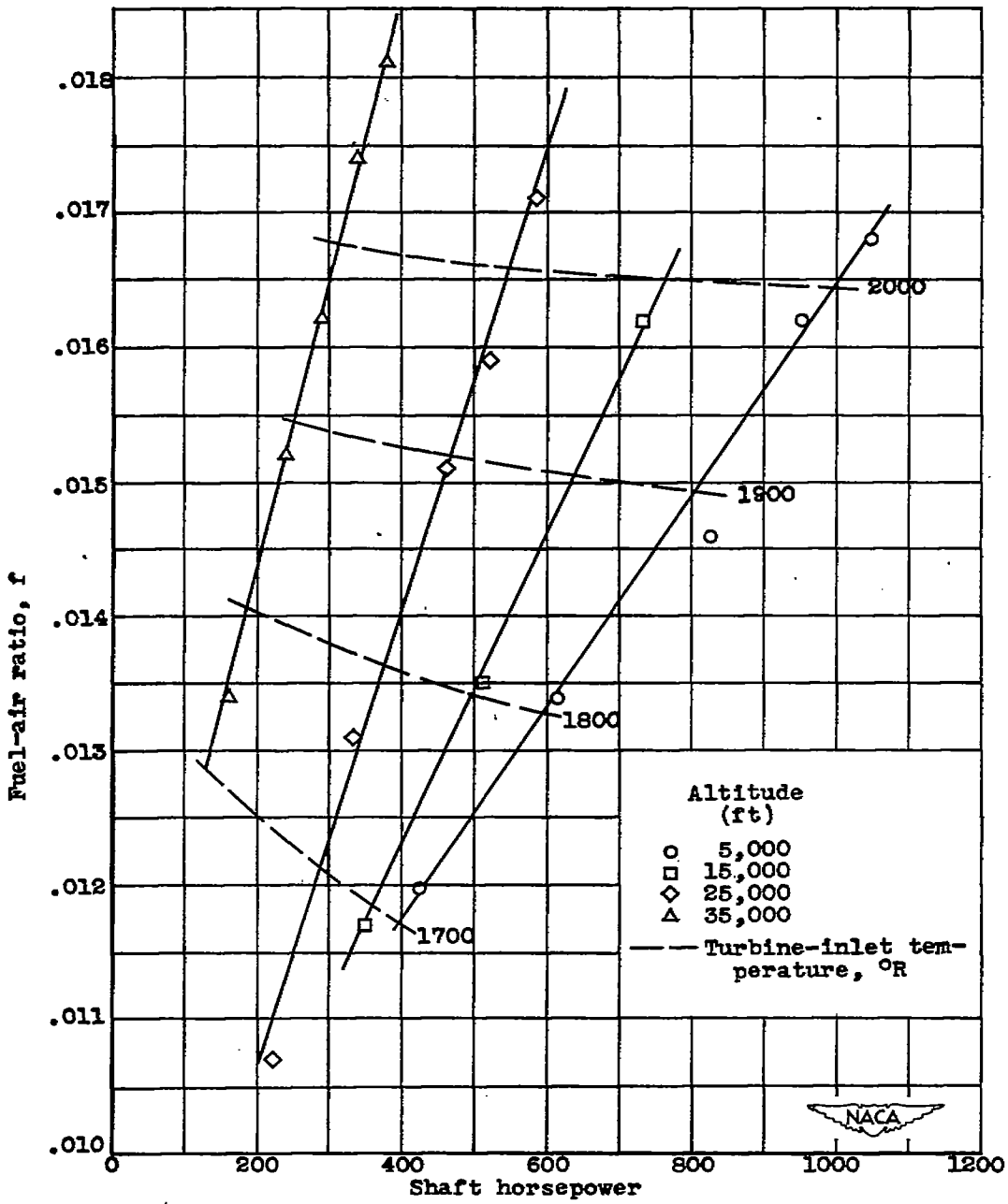

(d) Fuel-air ratio.

Figure 10. - Continued. Effect of shaft horsepower on engine-performance parameters at various altitudes. Engine speed, 13,000 rpm; compressor-inlet ram pressure ratio, 1.00.

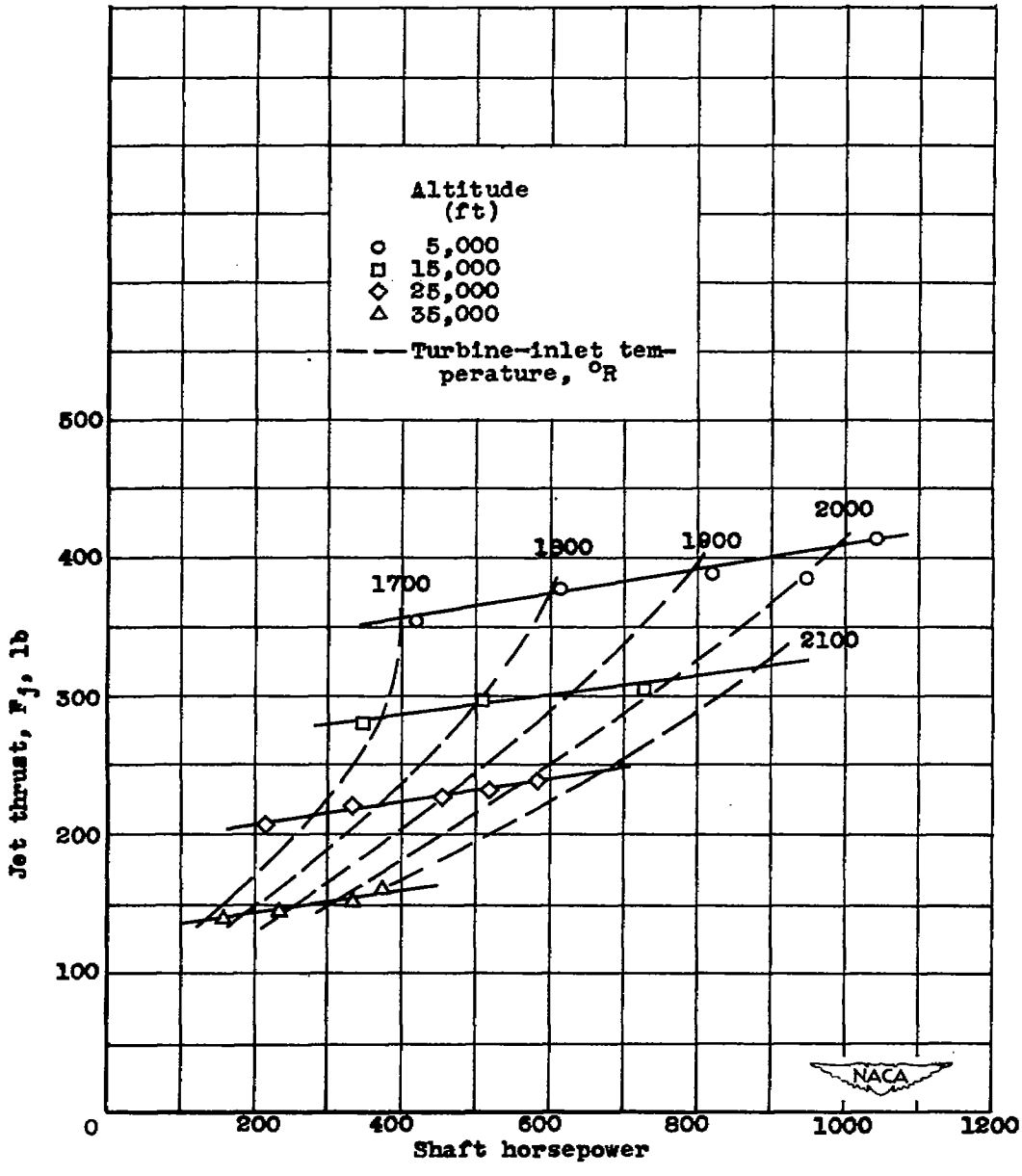

(e) Jet thrust.

Figure 10. - Continued. Effect of shaft horsepower on engine-performance parameters at various altitudes. Engine speed, 13,000 rpm; compressor-inlet ram pressure ratio, 1.00.

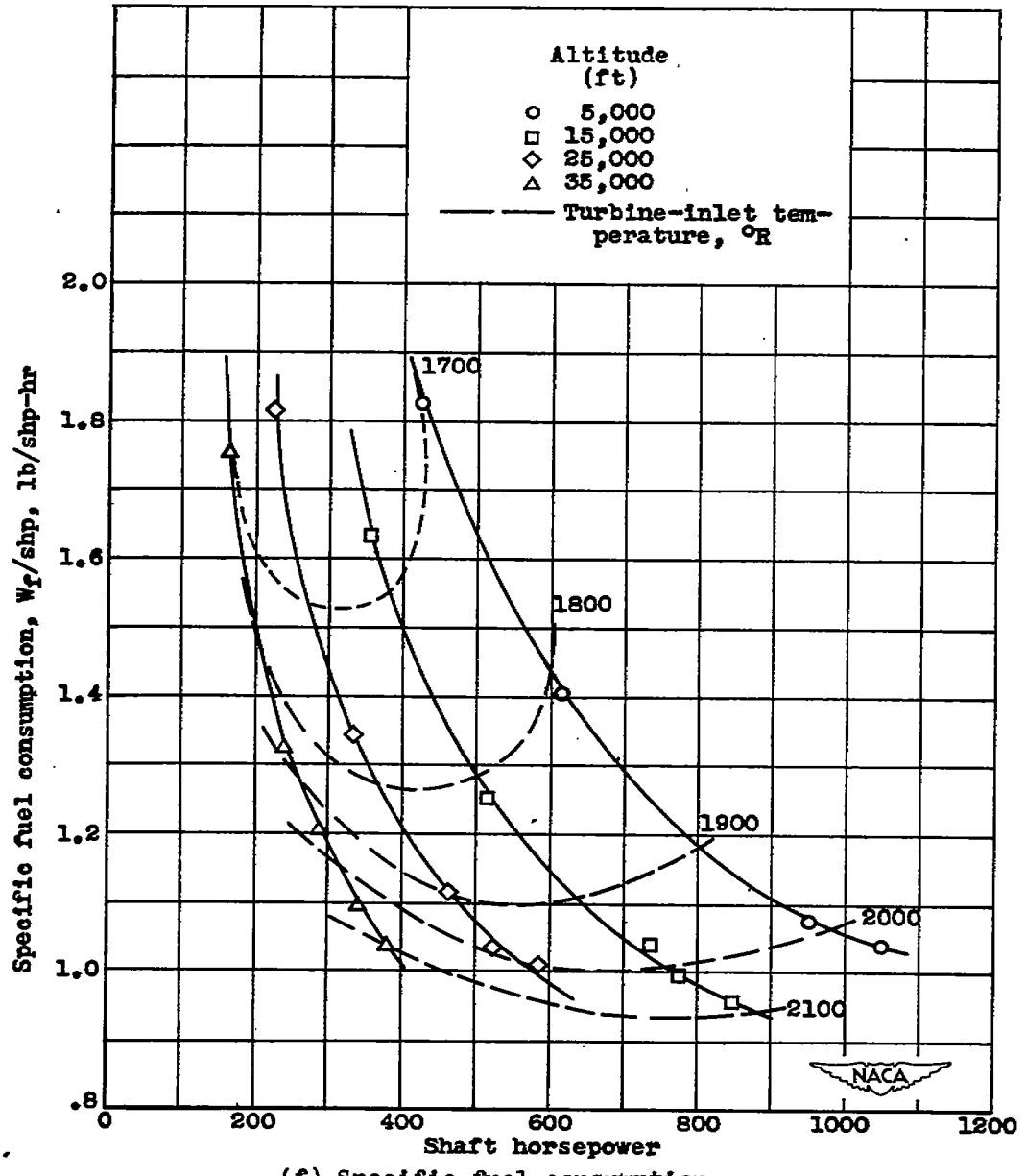

(f) Specific fuel consumption.

Figure 10. - Concluded. Effect of shaft horsepower on engine-performance parameters at various altitudes. Engine speed, 13,000 rpm; compressor-inlet ram pressure ratio, 1.00.

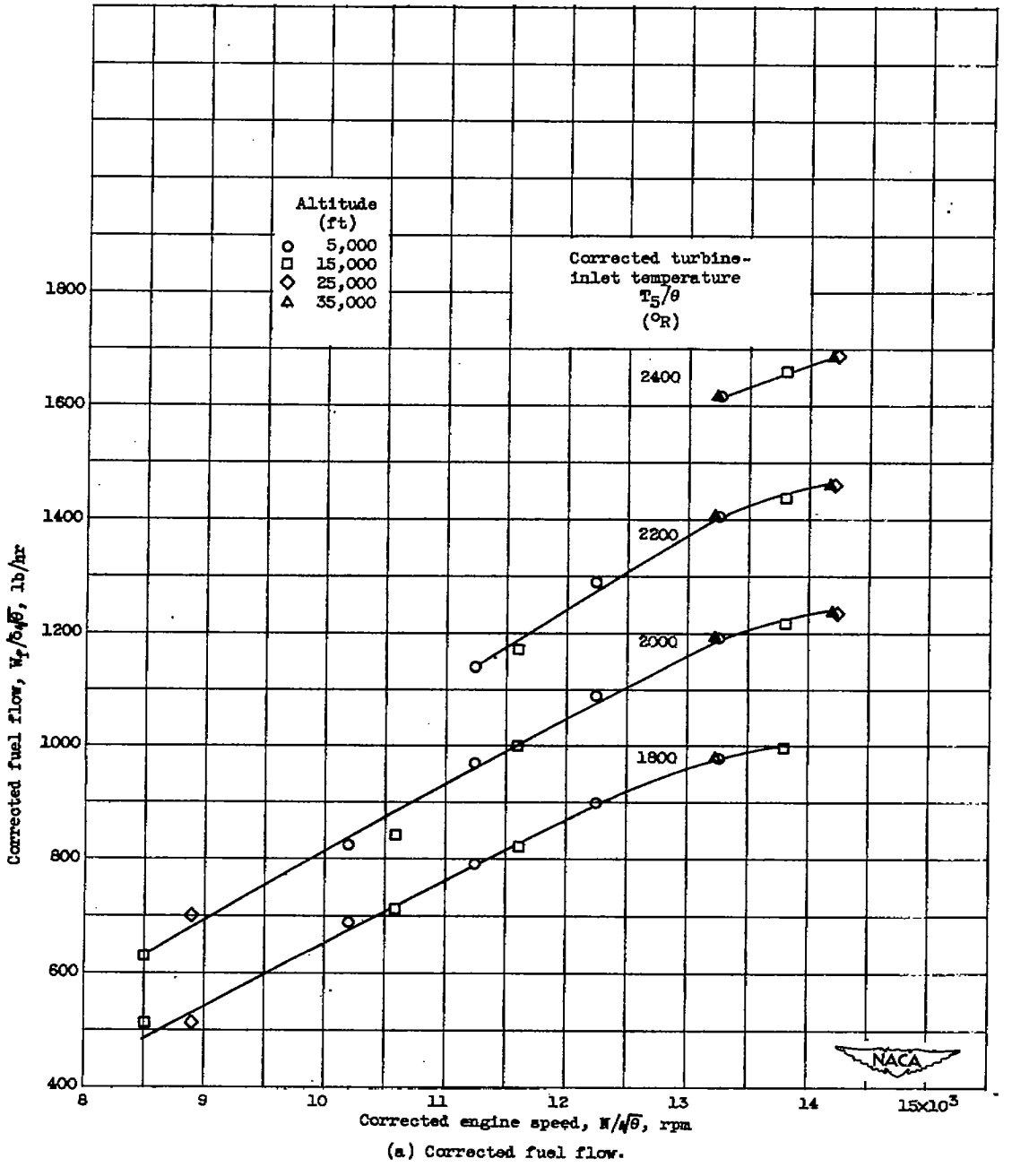

(a) Corrected fuel flow.

Figure 11. - Variation of corrected engine parameters with corrected engine speed. Compressor-inlet ram pressure ratio, 1.00.

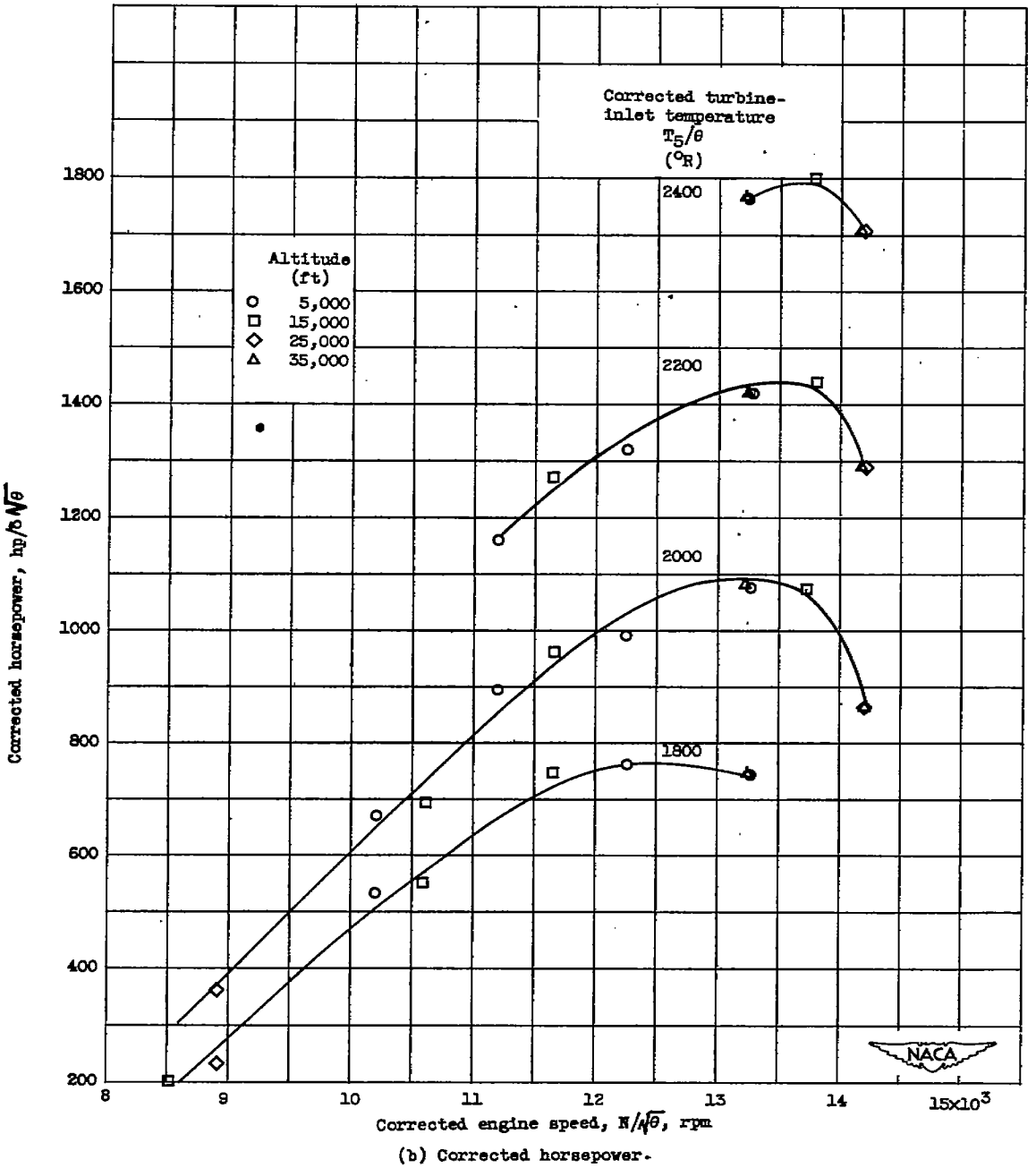

(b) Corrected horsepower.

Figure 11. - Continued. Variation of corrected engine parameters with corrected engine speed. Compressor-inlet ram pressure ratio, 1.00.

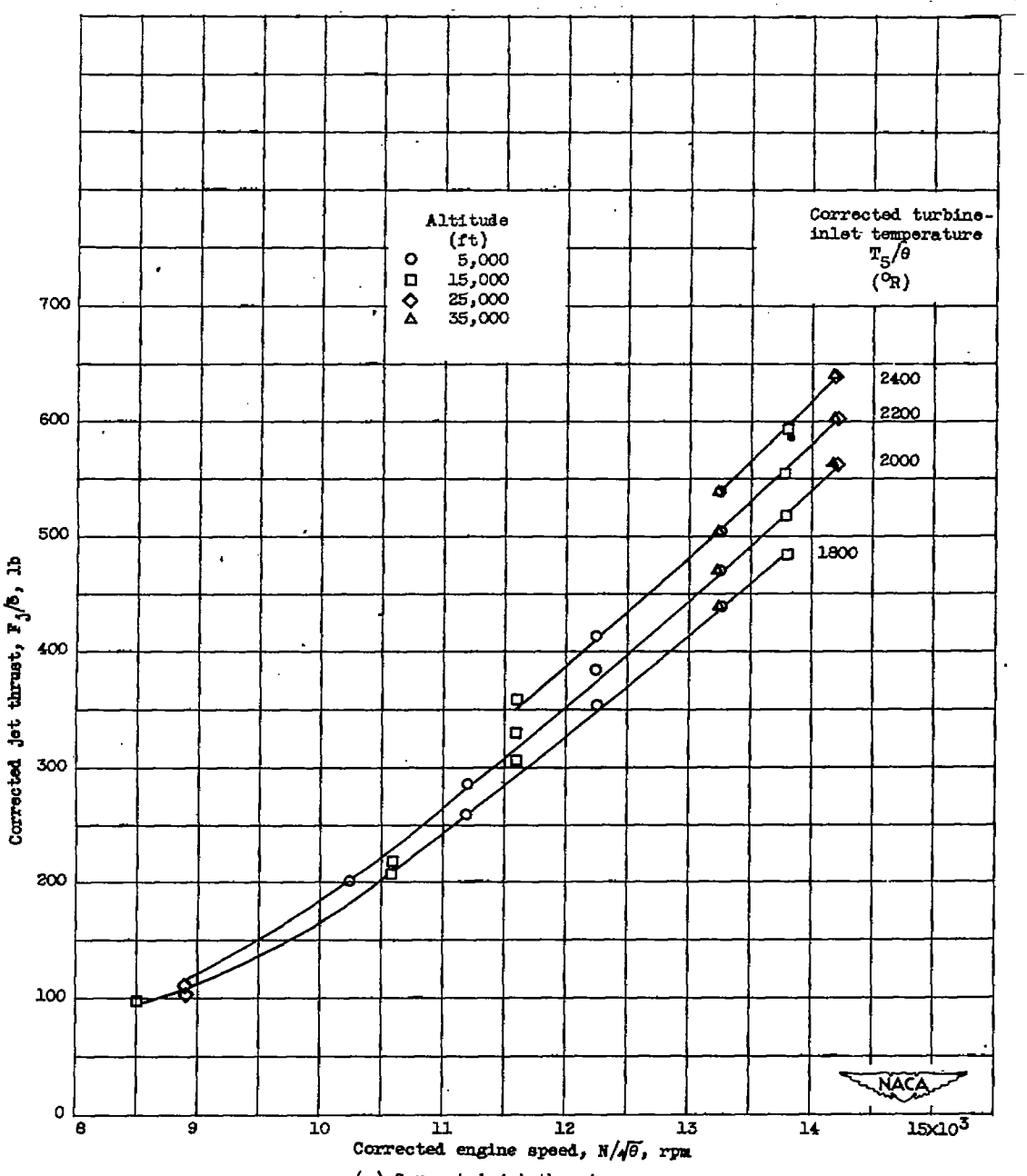

(c) Corrected jet thrust.

Figure 11. - Concluded. Variation of corrected engine parameters with corrected engine speed. Compressor-inlet ram pressure ratio, 1.00.

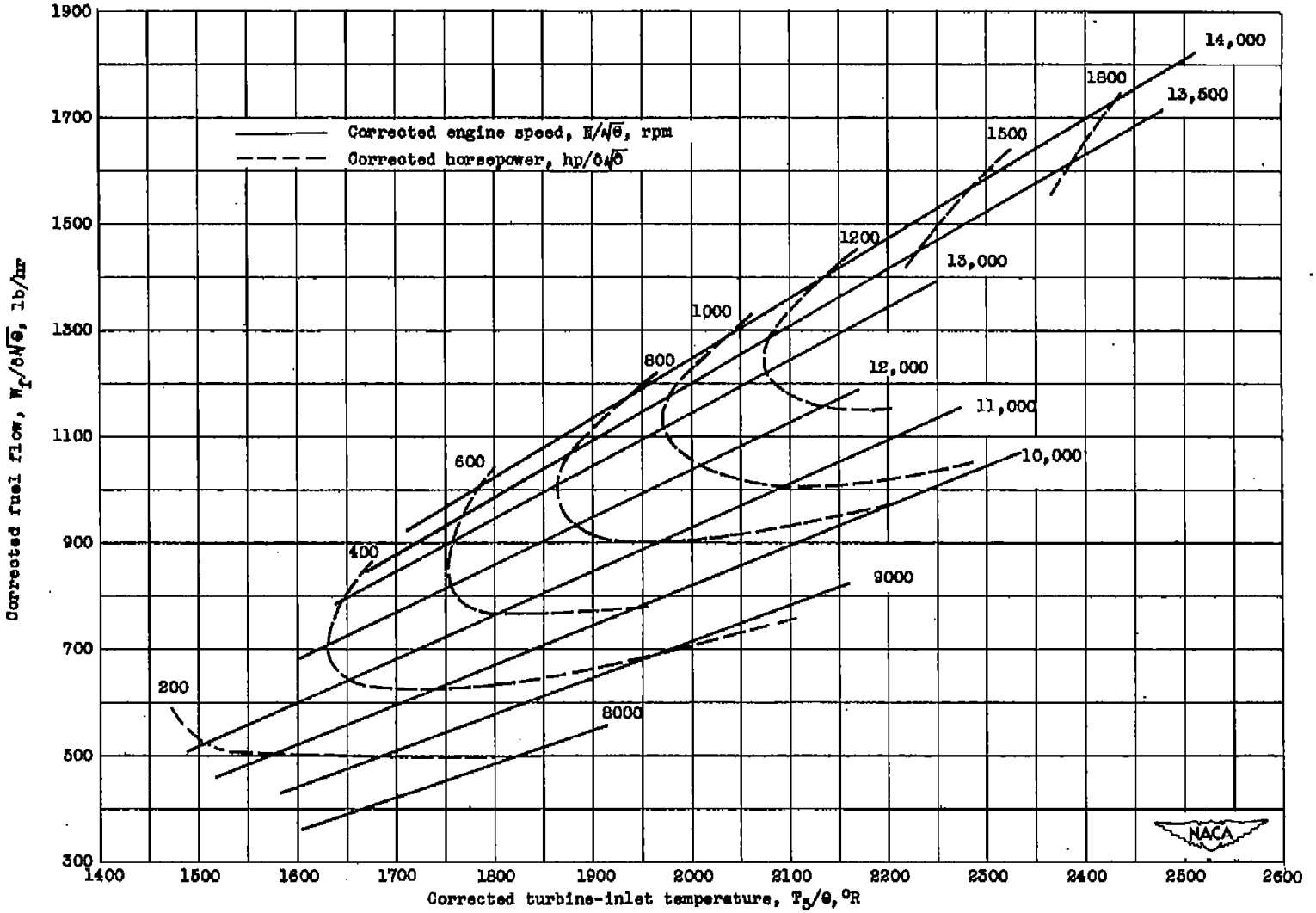

(a) Corrected fuel flow.

Figure 12. - Composite performance curves for turbine-propeller engine.

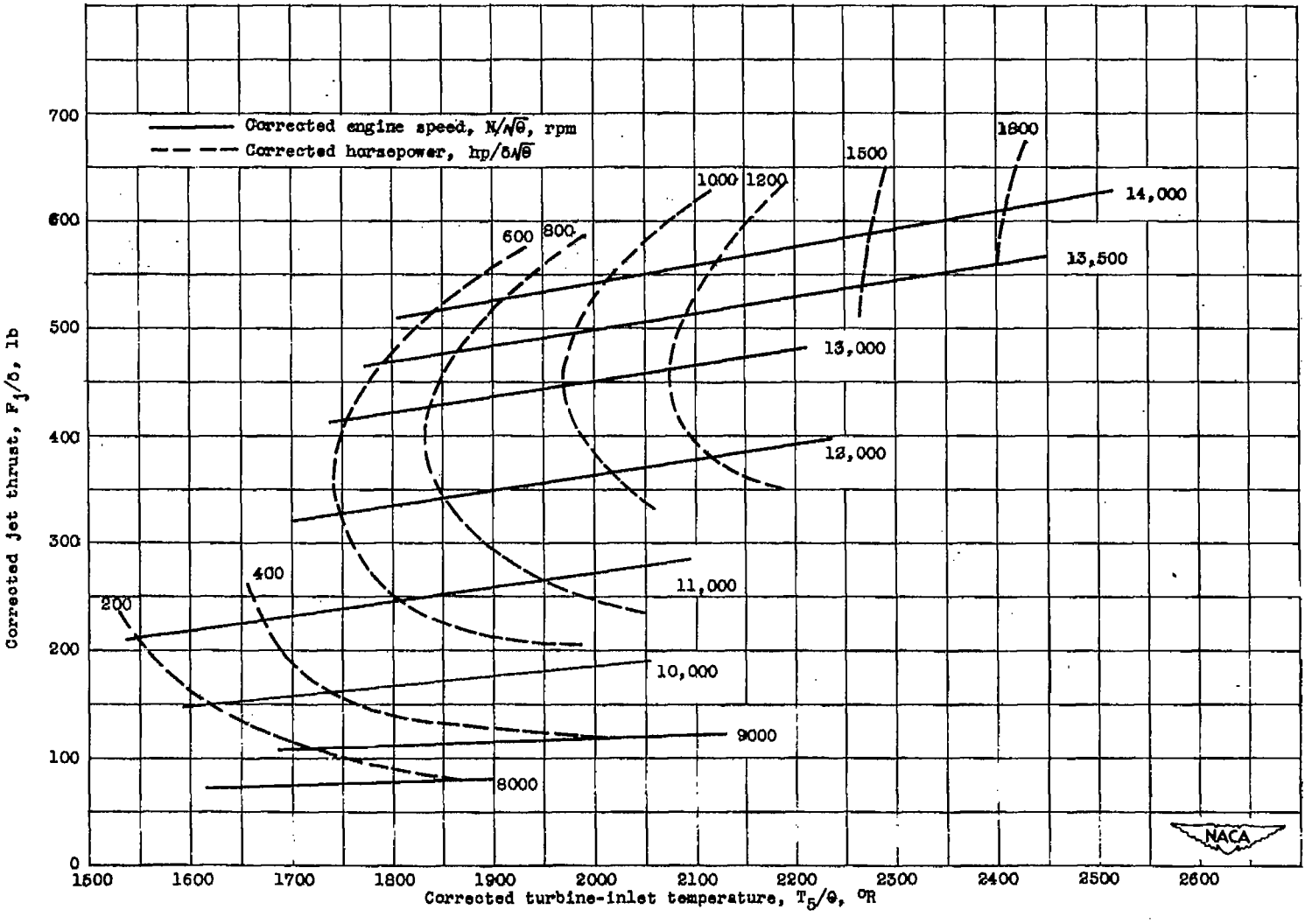

(b) Corrected jet thrust.

Figure 12. - Concluded. Composite performance curves for turbine-propeller engine.

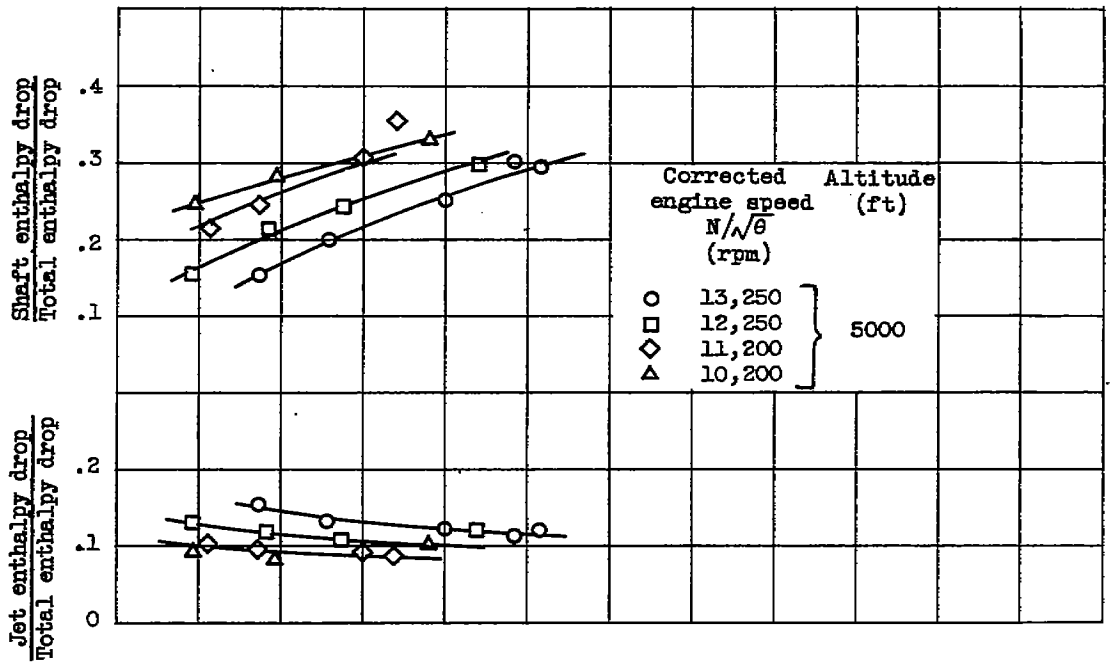

(a) Effect of engine speed at constant altitude.

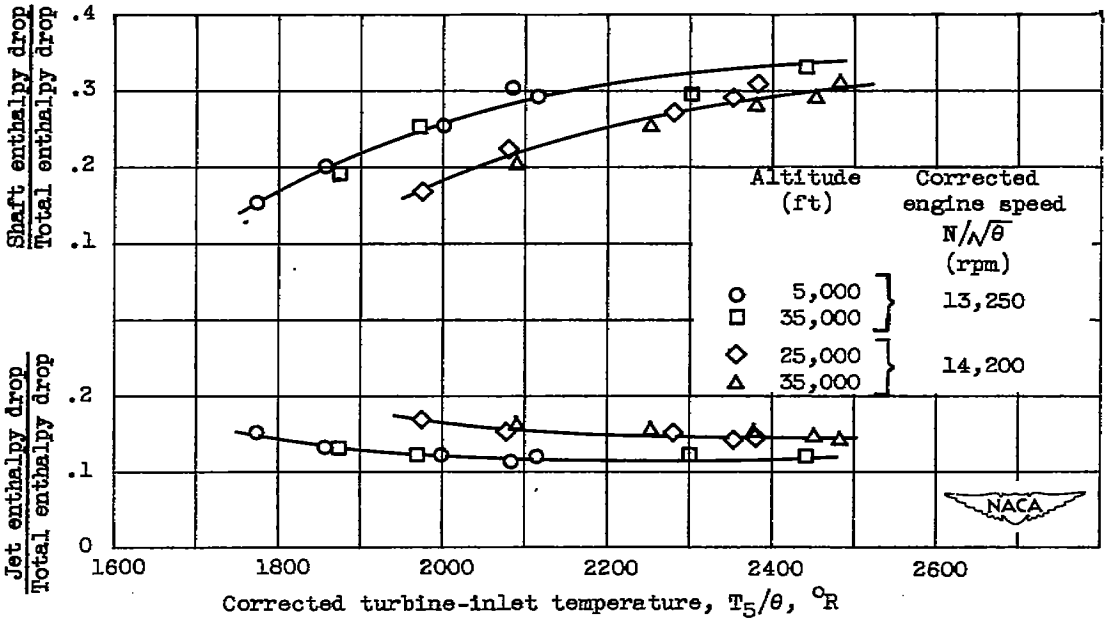

(b) Effect of altitude at two constant corrected engine speeds.

Figure 13. - Effect of engine speed and altitude on ratios of jet and propeller-shaft enthalpy drops to total enthalpy drop.

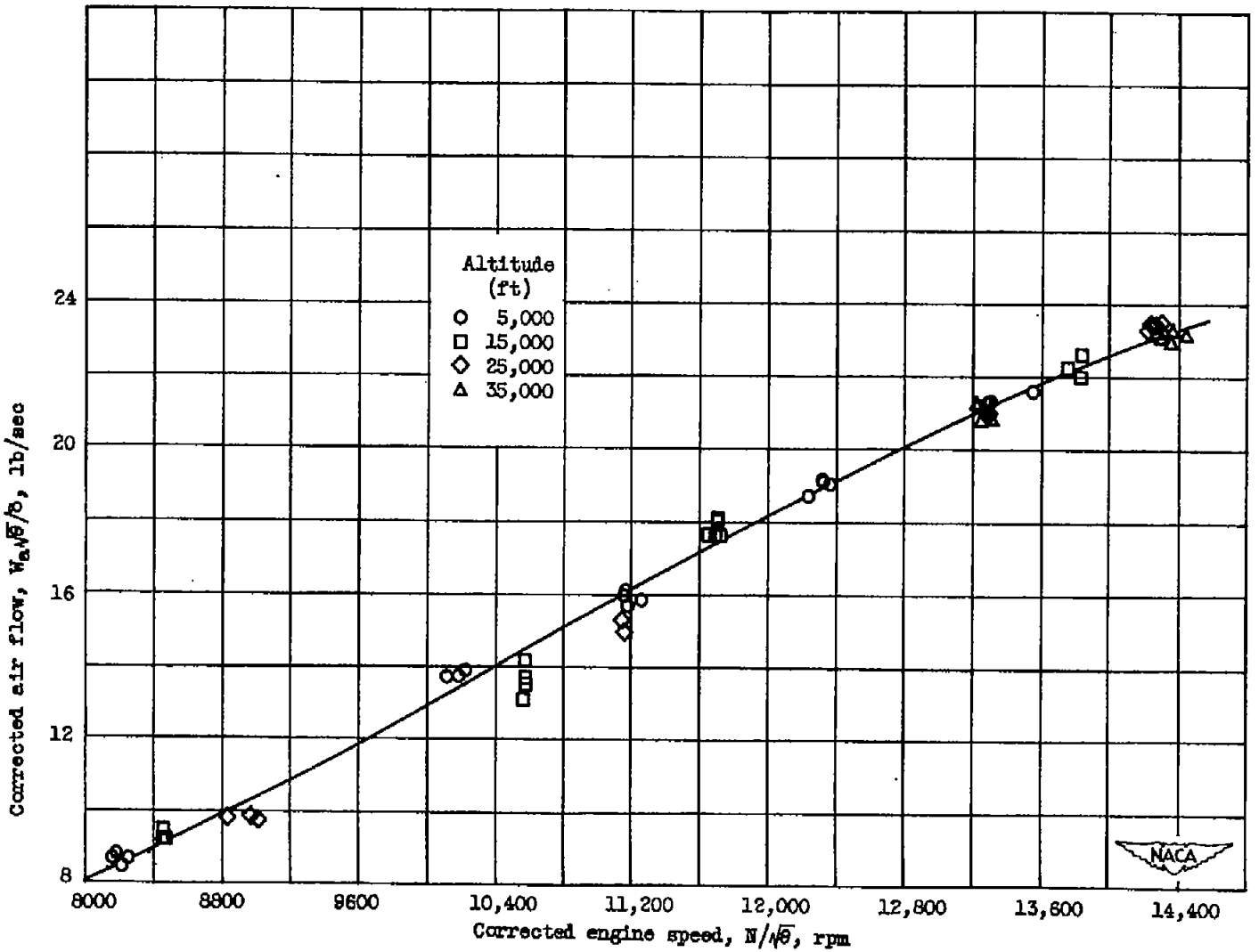

Figure 14. - Variation of corrected air flow with corrected engine speed. Compressor-inlet ram pressure ratio, 1.00.

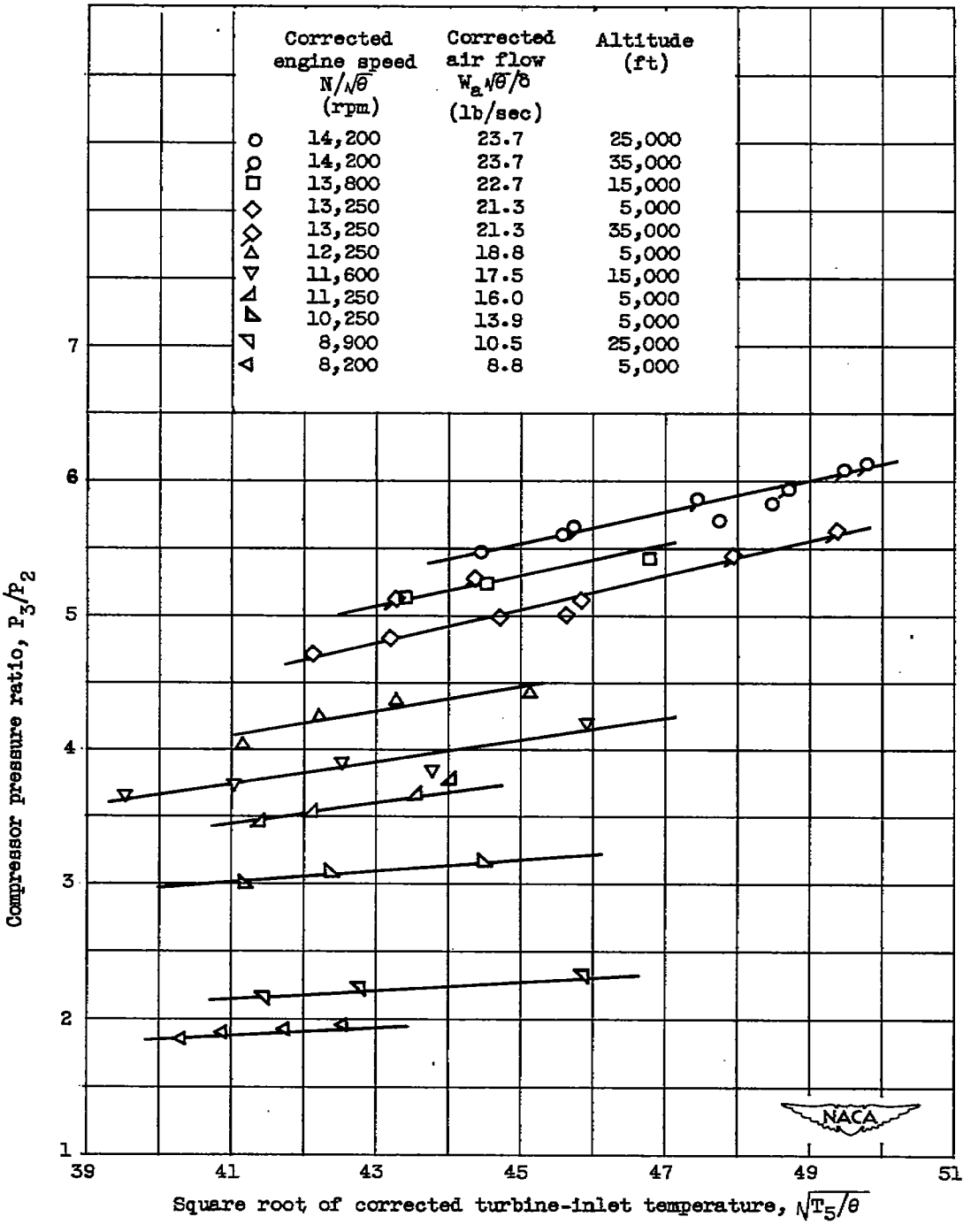

Figure 15. - Variation of compressor pressure ratio with corrected turbine-inlet temperature. Compressor-inlet ram pressure ratio, 1.00.

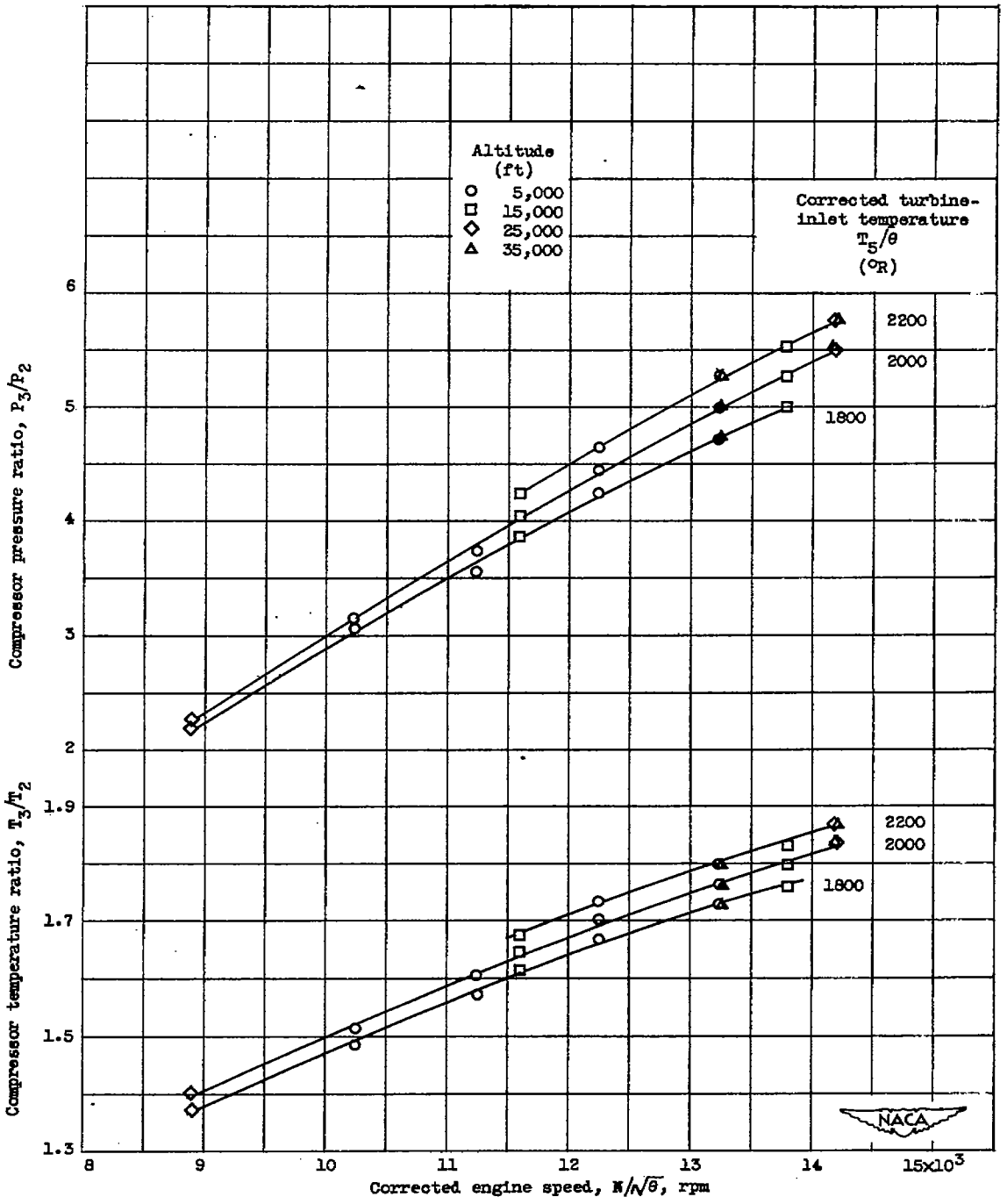

Figure 16. - Effect of altitude on compressor pressure and temperature ratios.

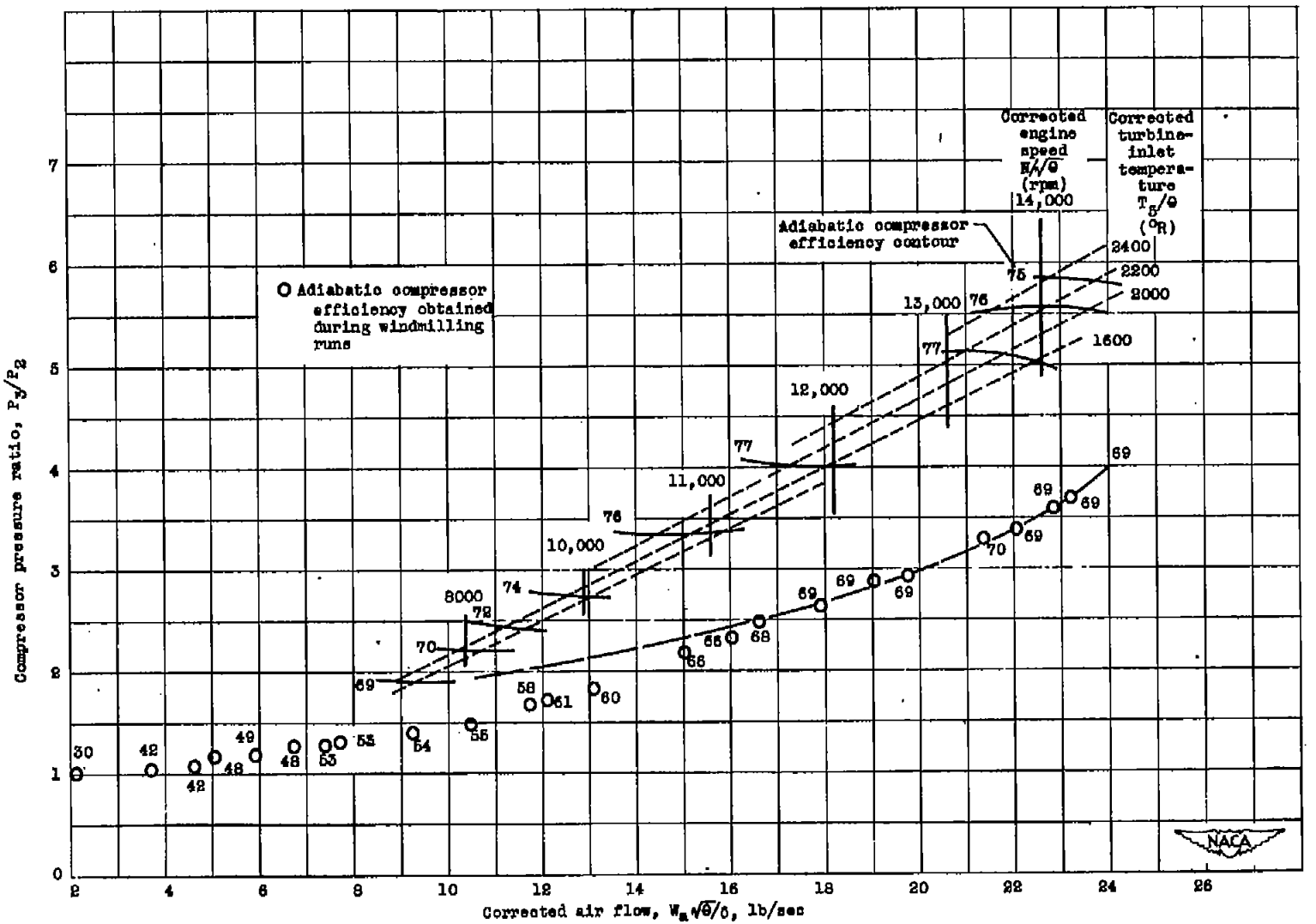

Figure 17. - Over-all compressor performance curves. Compressor-inlet ram pressure ratio, 1.00.

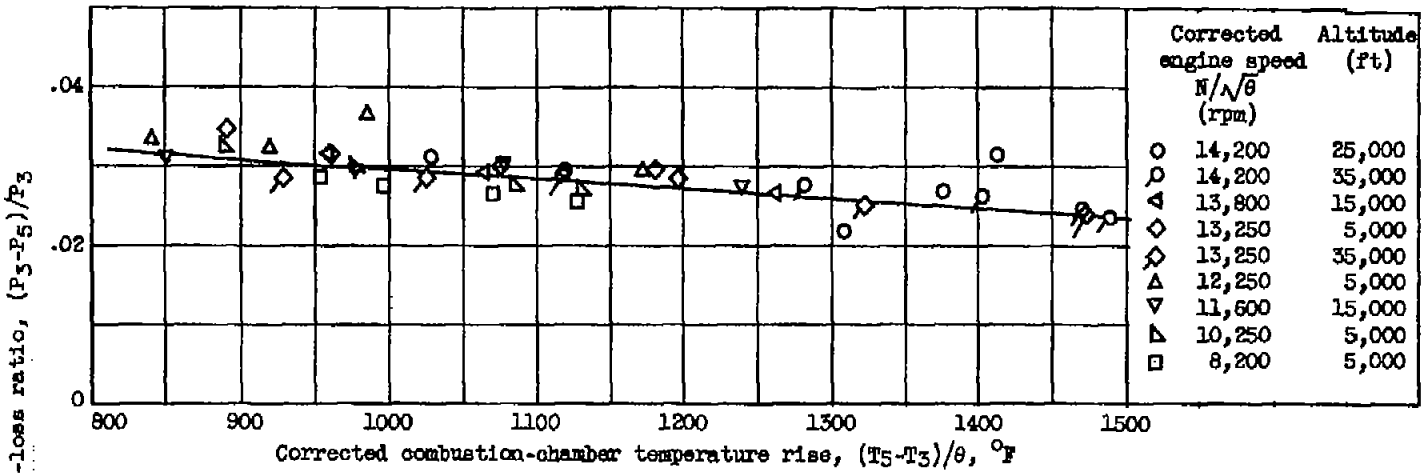

(a) Altitude effect.

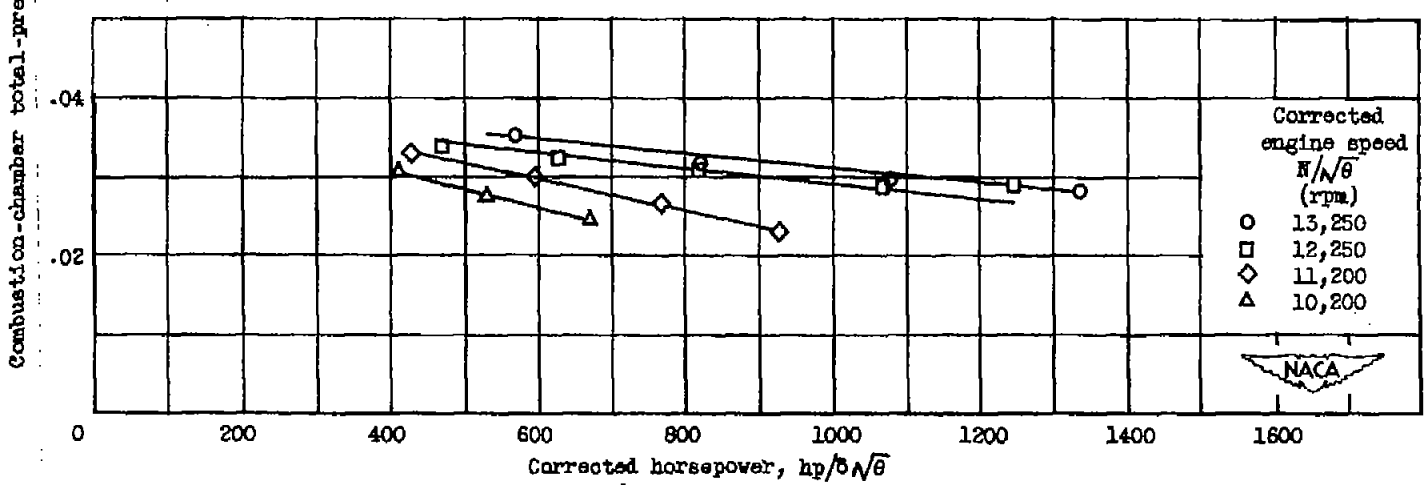

(b) Corrected engine speed effect. Altitude, 5000 feet.

Figure 18. - Variation of combustion-chamber total-pressure-loss ratio with corrected combustion-chamber temperature rise and corrected horsepower.

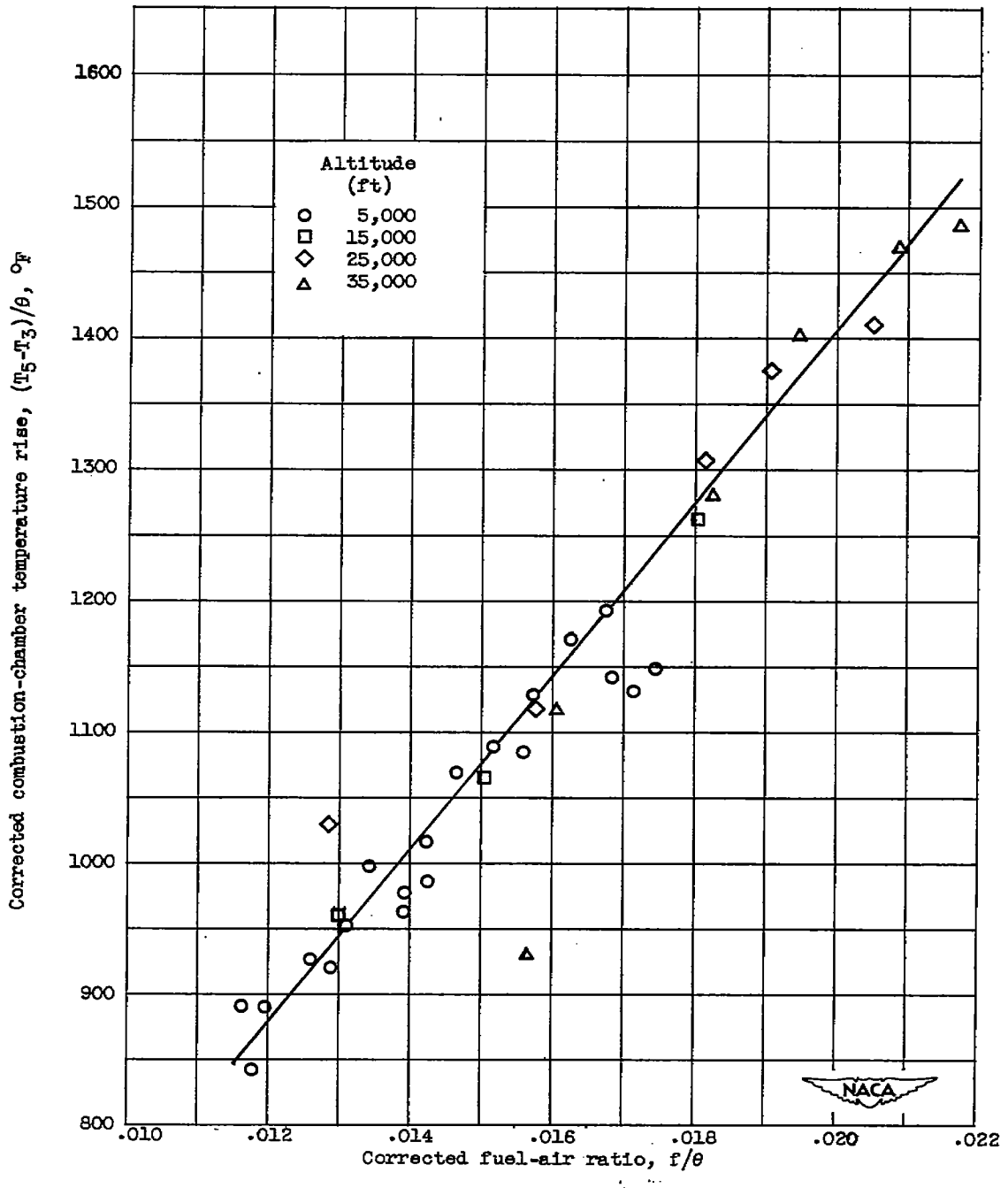

Figure 19. - Effect of altitude on engine combustion process. Corrected engine speed, 8200 to 14,200 rpm.

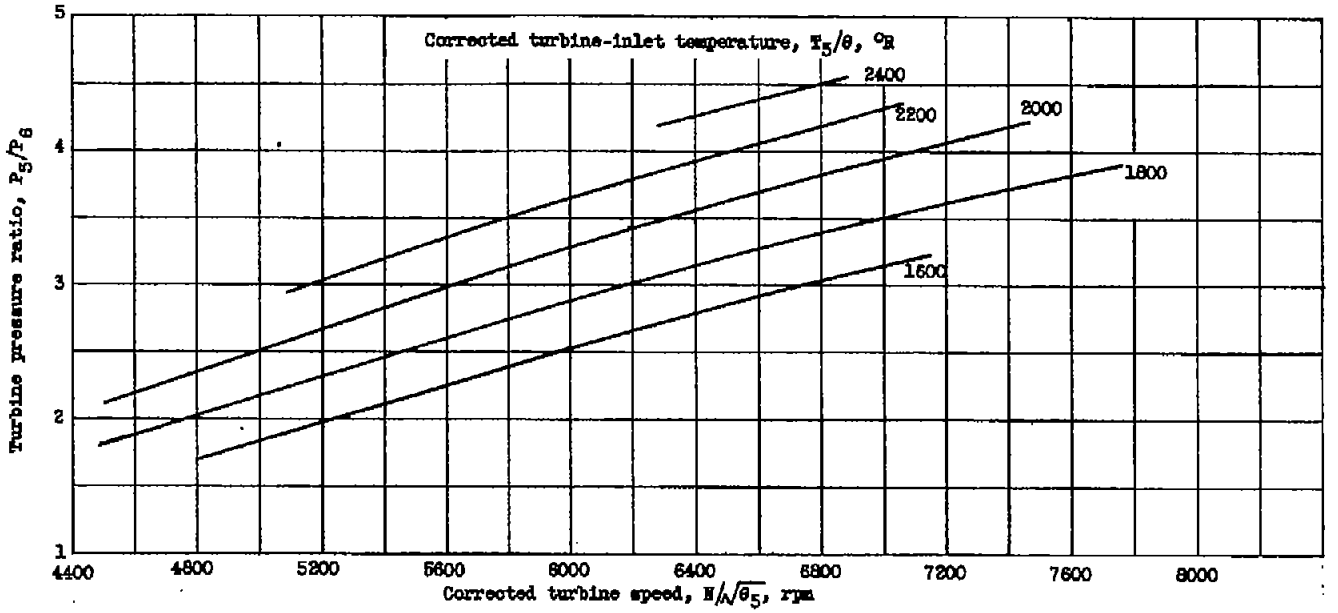

Figure 20. - Variation of turbine pressure ratio with corrected turbine speed at constant corrected turbine-inlet temperatures. Compressor-inlet ram pressure ratio, 1.00.

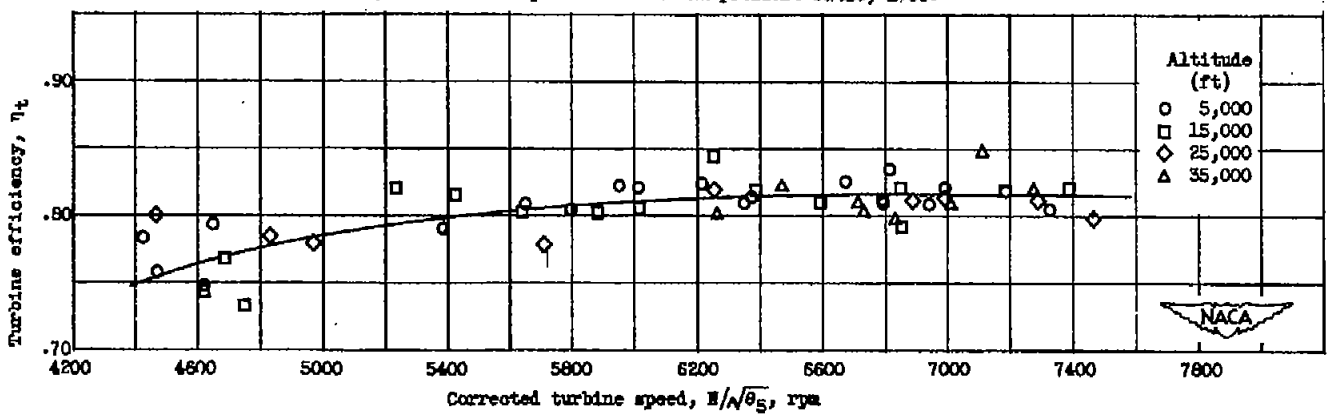

Figure 21. - Variation of turbine efficiency with corrected turbine speed. Compressor-inlet ram pressure ratio, 1.00.

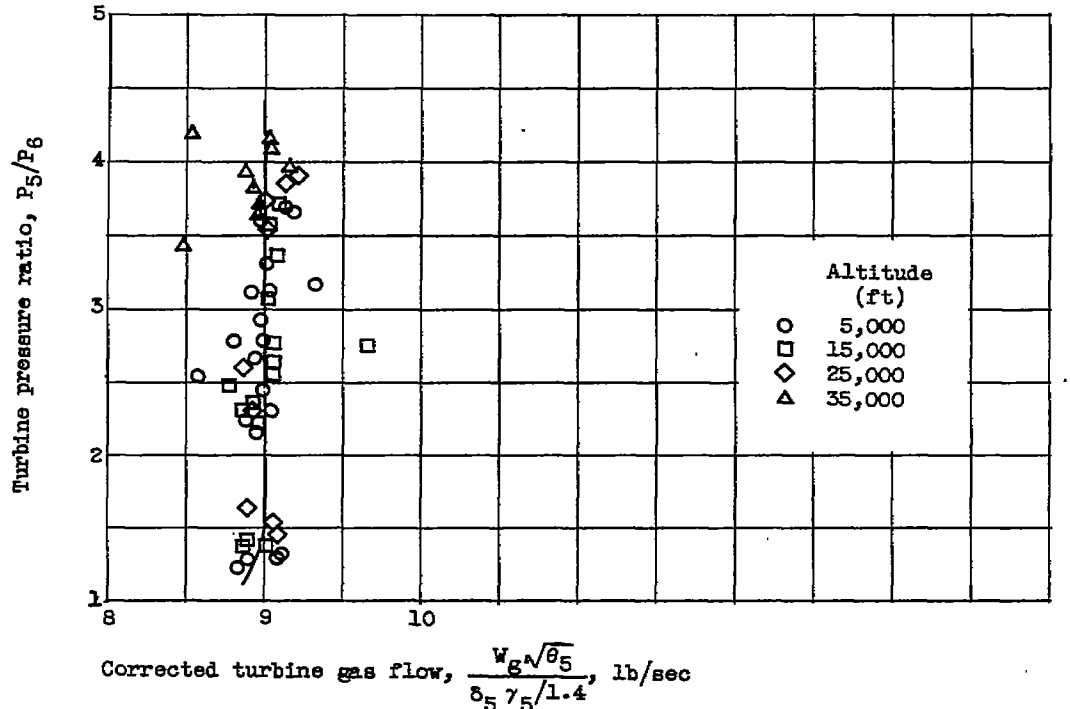

Figure 22. - Variation of turbine pressure ratio with corrected turbine gas flow. Compressor-inlet ram pressure ratio, 1.00.

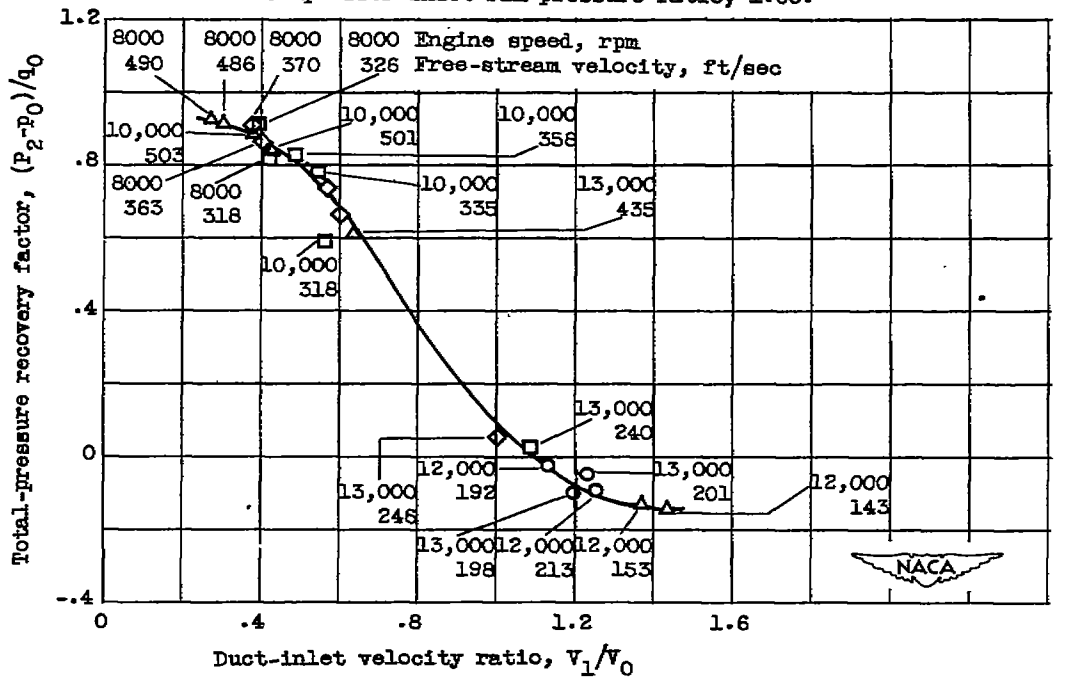

Figure 23. - Variation of induction-system total-pressure recovery with duct-inlet velocity ratio.

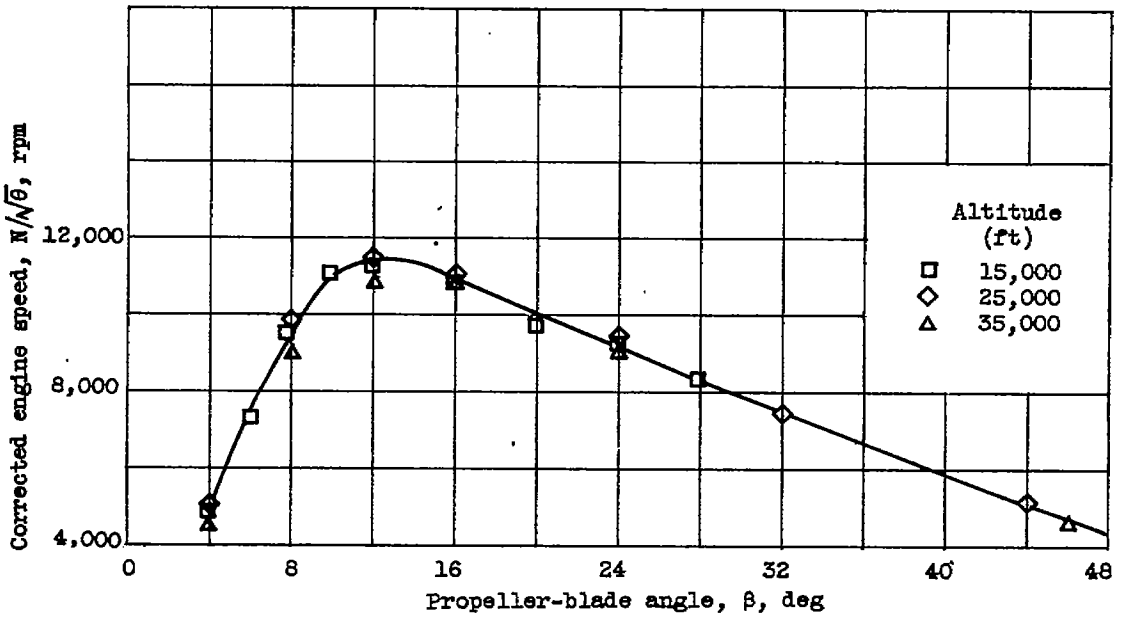

Figure 24. - Variation of corrected engine windmilling speed with propeller-blade angle. Flight Mach number, 0.285.

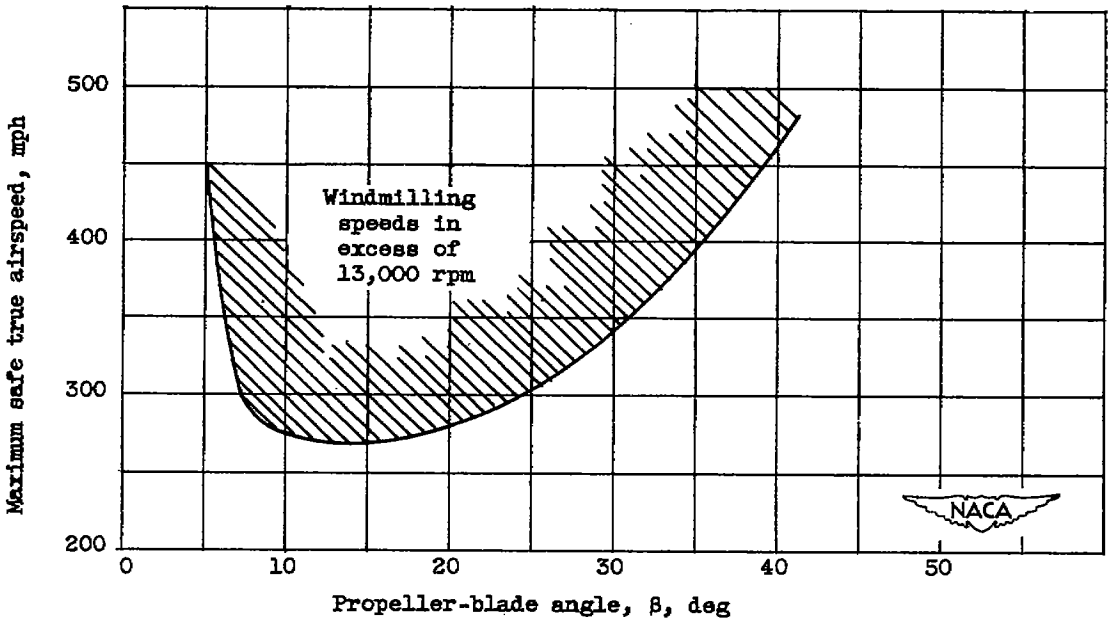

Figure 25. - Variation of maximum safe true airspeed with propeller-blade angle for windmilling engine.

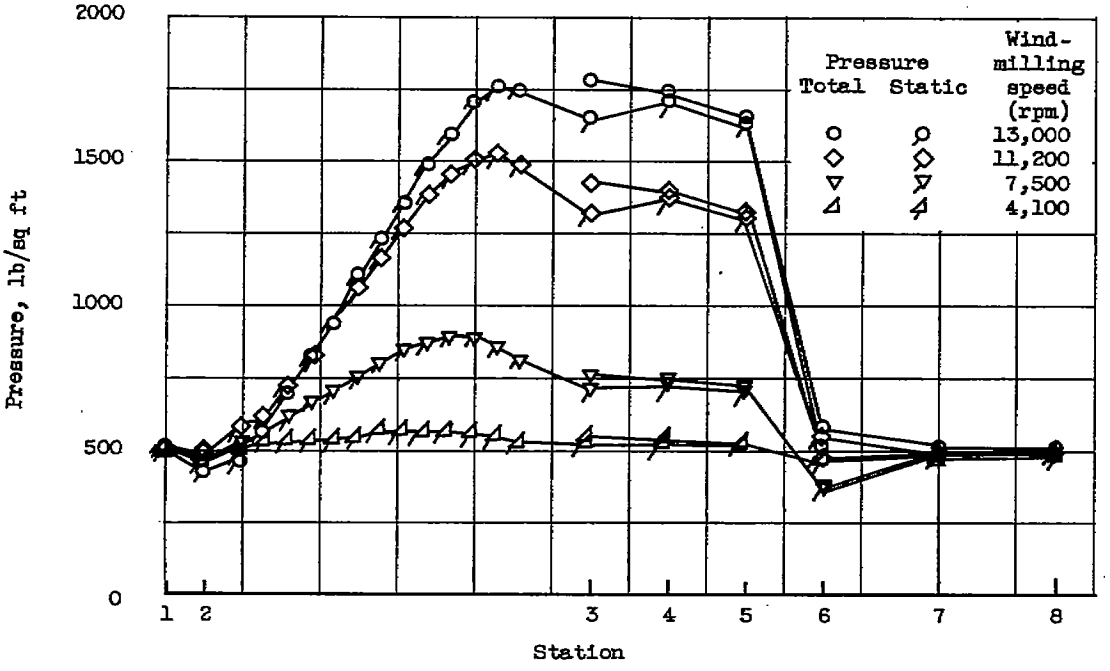

Figure 26. - Total and static pressures through engine at various windmilling speeds. Altitude, 35,000 feet; propeller-blade angle, 12°.

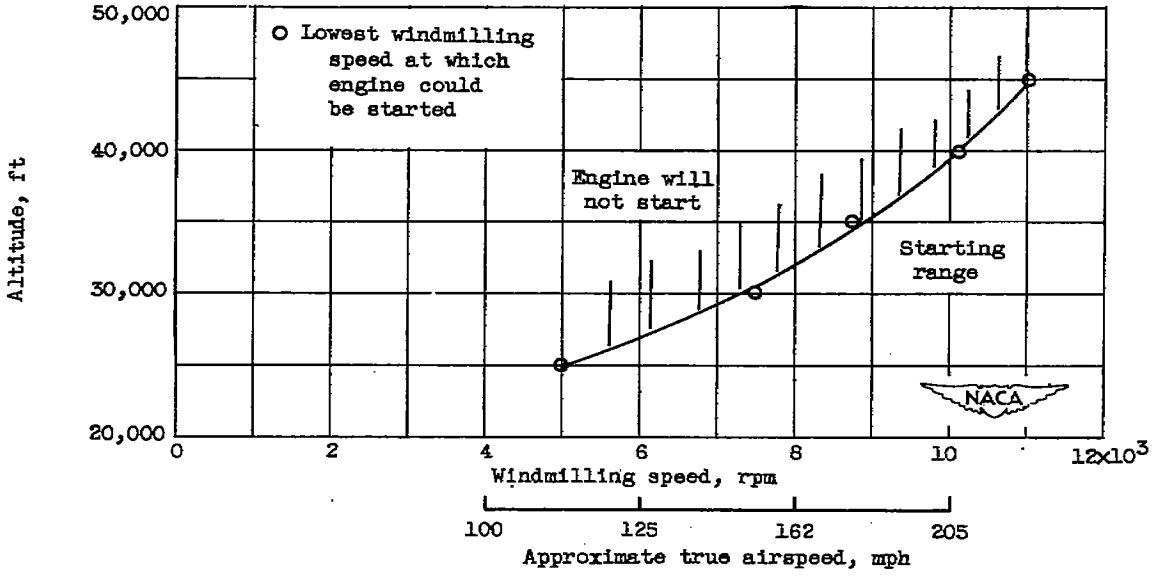

Figure 27. - Variation of minimum windmilling speed at which engine can be started with altitude.